

**Montana Water Center
Annual Technical Report
FY 2014**

Introduction

The Montana University System Water Center (MWC), located at Montana State University in Bozeman, was established by the Water Resources Research Act of 1964. In 2014, the Center's Director (Duncan Patten stepped down during 2014 and was replaced by Wyatt Cross) at Montana State University worked closely with the Assistant Director at Montana State University and the Associate Directors from Montana Tech of the University of Montana - Butte as well the University of Montana - Missoula , to coordinate statewide water research and information transfer activities. This is all in keeping with the Center's mission to investigate and resolve Montana's water problems by sponsoring research, fostering education of future water professionals and providing outreach to water professionals, water users and communities.

To help guide the Center's water research and information transfer programs and to help develop research priorities and assess research proposals the Montana Water Center depends on advice from members of its advisory council. In 2014 the Associate Director William Woessner at the University of Montana - Missoula stepped down. Andrew Wilcox at the University of Montana was selected as the new Associate Director for FY 2015. During the 2014 research year, the Montana Water Research Advisory Council members were:

Duncan Patten and Wyatt Cross, MWC Director; Stephanie McGinnis, MWC Assistant Director; John LaFave, MWC Associate Director, Montana Tech of the University of Montana, Montana Bureau of Mines; William Woessner, MWC Associate Director ,University of Montana; John Kilpatrick, Director - Montana Water Science Center, U.S. Geological Survey; Bonnie Lovelace, Water Protection Bureau Chief Montana Department of Environmental Quality; Tom Pick, Natural Resource and Conservation Service (now retired); Jeff Tiberi, Montana Association of Conservation Districts, Executive Director; Kathleen Williams, Montana Legislature (Water Specialist); and Laura Ziemer, Trout Unlimited.

We have started selection of new advisory council members for FY 2015.

Research Program Introduction

The Montana Water Center funded two faculty seed grant projects and six graduate student fellowship projects in 2014 with USGS funds. Each faculty research project is required to directly involve students in the field and/or with data analysis and presentations. Below is a brief statement of the researcher's and students' work.

Dr. Paul Stoy of Montana State University received an award of \$4,080 to study "Improving accessibility to satellite soil moisture measurements: Linking SMOS data retrievals to ground measurements in Montana". A report from this project is presented later in this annual report.

Kayan Ostovar of Rocky Mountain College received an award of \$11,475 to study "Contaminants monitoring and natal dispersal of ospreys along the Yellowstone River". A report from this project is presented later in this annual report.

Douglas Brugger, at the University of Montana was awarded a \$2,000 student fellowship to study "The Impact of Irrigation on the Hydrologic Cycle under Low Water Availability". A report from this project is presented later in this annual report.

Emily Clark, at Montana State University was awarded a \$2,000 student fellowship to study "Thresholds of Hydrologic Connectivity: Shallow Water Table Development at the Hillslope Scale". A report from this project is presented later in this annual report.

Elizabeth Harris, at Montana State University was awarded a \$2,000 student fellowship to study "Seasonal Timing of Evapotranspiration and the Effect on Soil Moisture and Water Availability for Groundwater Recharge with Different Crop Rotation Practices". A report from this project is presented later in this annual report.

Aiden Johnson, at Montana State University was awarded a \$2,000 student fellowship to study "Estimating Evapotranspiration at the Regional Scale: An Energy Balance Approach". A report from this project is presented later in this annual report.

Justin Martin, at Montana State University was awarded a \$2,000 student fellowship to study "Precipitation and topographic controls over montane forest transpiration". A report from this project is presented later in this annual report.

April Sawyer, at the University of Montana was awarded a \$2,000 student fellowship to study "Conditions necessary to maintain chute-cutoff morphology in meandering gravel-bed rivers". A report from this project is presented later in this report.

The Montana Water Center selected three faculty seed grant projects and four graduate student fellowship projects to fund in 2015 with USGS 104(b) research program funds administered by the Montana Water Center. The selected faculty grants are:

Jamie McEvoy of Montana State University will receive an award of \$14,886 to study "Assessing the capacity of natural infrastructure to increase water storage, reduce vulnerability to floods, and enhance resiliency to climate change".

Ellen Lauchnor of Montana State University will receive an award of \$15,000 to study "Nitrifying wastewater biofilms and the influence of emerging contaminants".

Research Program Introduction

Benjamin Poulter of Montana State University will receive an award of \$5,832 to study "Designing scenarios for hydrologic resilience in the Upper Missouri Headwaters with integrated ecosystem models".

The selected student fellowships are:

Sarah Benjaram, at Montana State University will receive a \$1,000 student fellowship to study "Climatic and geomorphologic influences on soil development and transport in the Bitterroot and Sapphire Mountains, Montana, USA".

Michael Jahnke, at University of Montana will receive a \$1,000 student fellowship to study "Sediment routing in steep mountain streams to understand hillslope-channel connectivity".

Miranda Margetts, at Montana State University will receive a \$1,000 student fellowship to study "Enhancing Tribal Environmental Health Literacy: Developing a toolkit to improve community understanding of rights and responsibilities regarding water quality".

Taylor Wilcox, at University of Montana will receive a \$909 student fellowship to study "Environmental DNA to evaluate individual variation in rainbow trout spawning date".

Improving accessibility to satellite soil moisture measurements: Linking SMOS data retrievals to ground measurements in Montana

Basic Information

Title:	Improving accessibility to satellite soil moisture measurements: Linking SMOS data retrievals to ground measurements in Montana
Project Number:	2014MT284B
Start Date:	3/1/2014
End Date:	2/28/2016
Funding Source:	104B
Congressional District:	MT 1
Research Category:	Climate and Hydrologic Processes
Focus Category:	Surface Water, None, None
Descriptors:	None
Principal Investigators:	Paul C Stoy

Publications

There are no publications.

Improving accessibility to satellite soil moisture measurements: Linking SMOS data retrievals to ground measurements in Montana

An interim report for the Montana Water Center

Paul C. Stoy

April 31, 2015

The aridity index of Montana has increased over the past 50 years due to an increased atmospheric demand for water rather than a decrease in precipitation (Sheffield et al. 2006; Stoy 2013). Improved access to state-of-the-art observations of Montana water resources will enable managers to make informed decisions about our increasingly scarce water supply, and lessons learned in Montana may have benefits for other semiarid regions across the globe (Wallace and Batchelor 1997).

Plant growth is more sensitive to soil moisture than any other variable in the hydrologic cycle (Rodriguez-Iturbe and Porporato 2004). Soil moisture is conventionally measured at scales on the order of centimeters manually or using time domain reflectometry (TDR), but COSMOS (Zreda et al. 2008) and satellite-based soil moisture measurements (see Table 1 in Ford, Harris, & Quiring, 2013) create new opportunities for studying soil moisture across larger scales in space. COSMOS measures soil moisture using neutron backscatter on spatial scales of hundreds of meters and at depths on the order of 5 – 30 cm from a ground-based platform, and SMOS is a satellite measures the top centimeters of soil in 50 km footprints. It is unclear if these differences in spatial scale and location lead to important discrepancies in soil moisture estimates in Montana.

The present project funded 2.3 months of graduate student summer support to: 1) Download and process data from the European Soil Moisture and Ocean Salinity (SMOS)

satellite; 2) Validate SMOS data for agricultural regions of Montana; 3) Provide public soil moisture data access. The proposed project is designed to align with Montana Water Center priority issues by fostering student involvement, assisting new faculty members, providing seed funding with potential for larger programs, and conducting research relevant to MT water challenges.

As noted, SMOS has partial spatial coverage of the terrestrial surface and provides soil moisture estimates over the first few centimeters of soil in 50 km swaths. As a consequence, there is often a spatial disconnection between the area of SMOS measurement and area of interest. We compared SMOS data against TDR measurements from a site in the Judith Basin near Moore, MT, and against COSMOS observations near Fort Peck, MT (Figure 1).

Observations reveal a substantial mismatch between SMOS and TDR measurements in the Judith Basin (Figure 1) with an average difference of $0.2 \text{ m}^3 \text{ m}^{-3}$ or more, and a close match between SMOS and COSMOS observations at Fort Peck, usually within $0.05 \text{ m}^3 \text{ m}^{-3}$ or less (Figure 2). The mechanisms that underlie these differences is unclear; the SMOS footprint encompasses both the Judith Basin TDR measurements (Figure 3) and Fort Peck COSMOS observations (Figure 4). The SMOS center point and COSMOS sensors are separated by only 3.8 km at Fort Peck on similar land cover (Figure 5). TDR measurements and SMOS center points are separated by 7.5 km in the Judith Basin and both are on agricultural land. The SMOS pixel in the Judith Basin overlaps with the Big Snowy Mountains, although one would expect springtime soil moisture measurements to be higher than the observed SMOS range of 0.05 to 0.35 during this period.

Observations suggest that SMOS observations may or may not intersect with TDR and COSMOS observations, albeit for reasons that are unclear. SMOS captures observations across a large 50 km pixel with a three day overpass, and the characteristic spatial and temporal scales of soil moisture variability may be much finer than its native measurement resolution (Katul et al. 2007). It is likewise unclear how to best communicate such observations outside of making data from the Judith Basin TDR observations publically available as COSMOS already is (<http://cosmos.hwr.arizona.edu/Probes/StationDat/048>). Further, the recently-launched Soil Moisture Active Passive (SMAP) mission reports data in smaller 10 km pixels every 2-3 days. Future efforts should use seek to validate publicly-available SMAP data rather than SMOS, which requires permissions and extensive processing, for an improved understanding of the variability of Montana's near-surface soil moisture resources for agricultural and water resource planning.

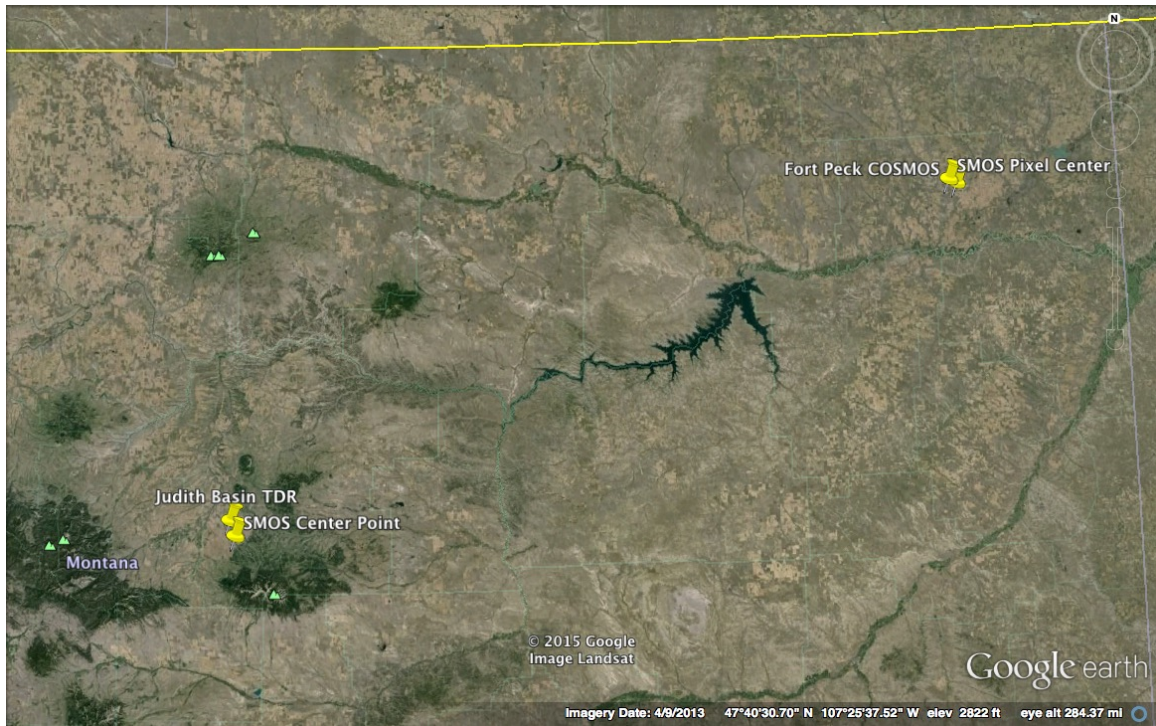


Figure 1: The location of Time Domain Reflectometry (TDR) and COSMOS observations in the Judith Basin and Fort Peck, MT compared against 50 km SMOS pixel center points. The vertical gray line is the Montana/North Dakota border and the yellow line is the US/Canada border.

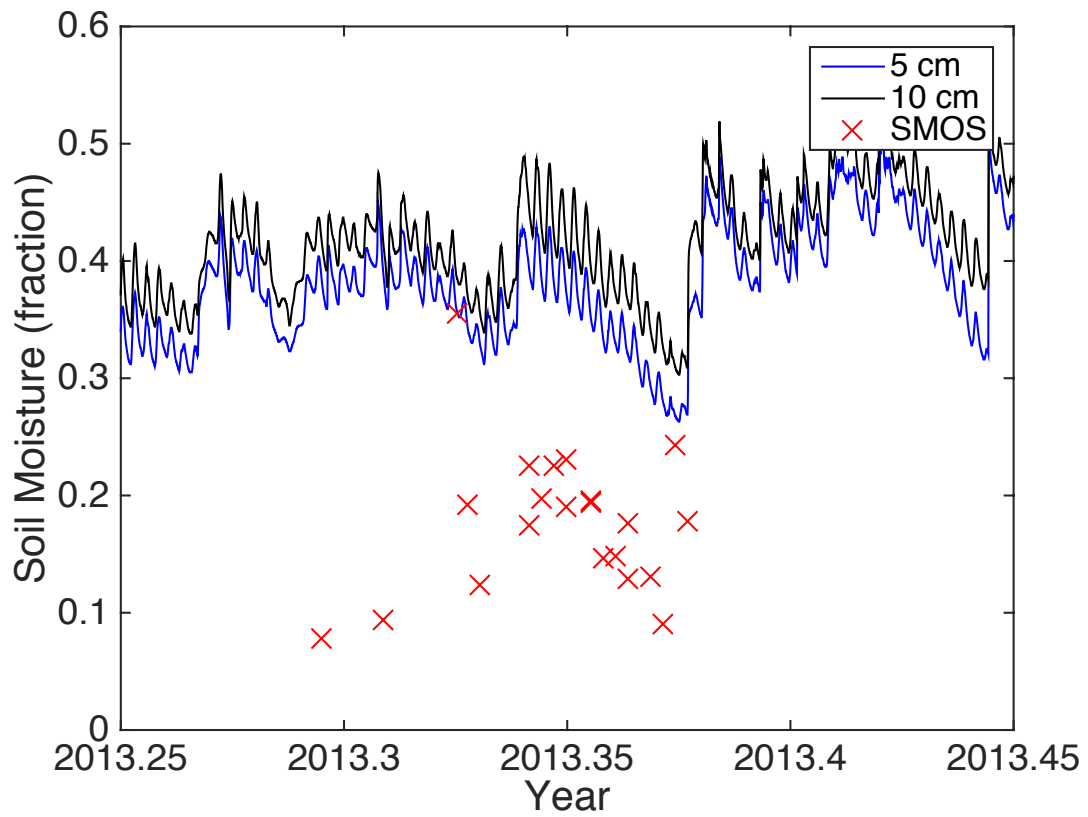


Figure 2: SMOS and time domain reflectometry (TDR) measurements in the Judith Basin near Moore, MT.

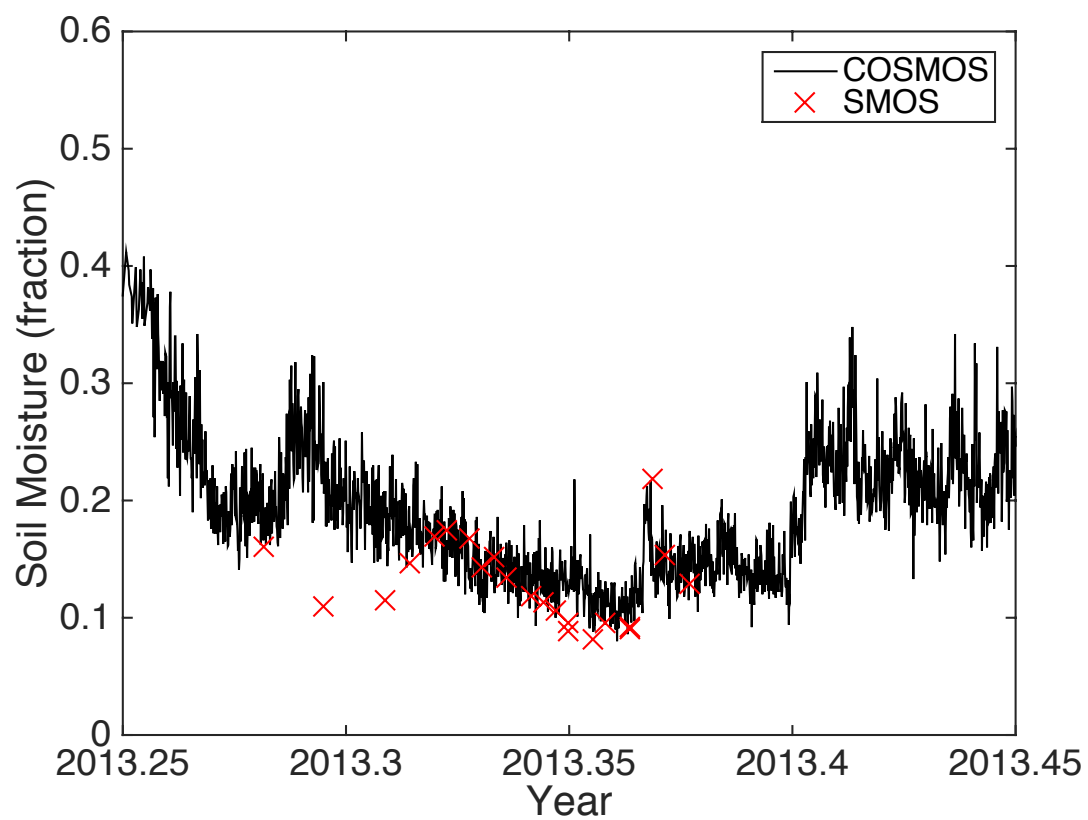


Figure 3: SMOS and COSMOS observations from sites near Fort Peck, MT.

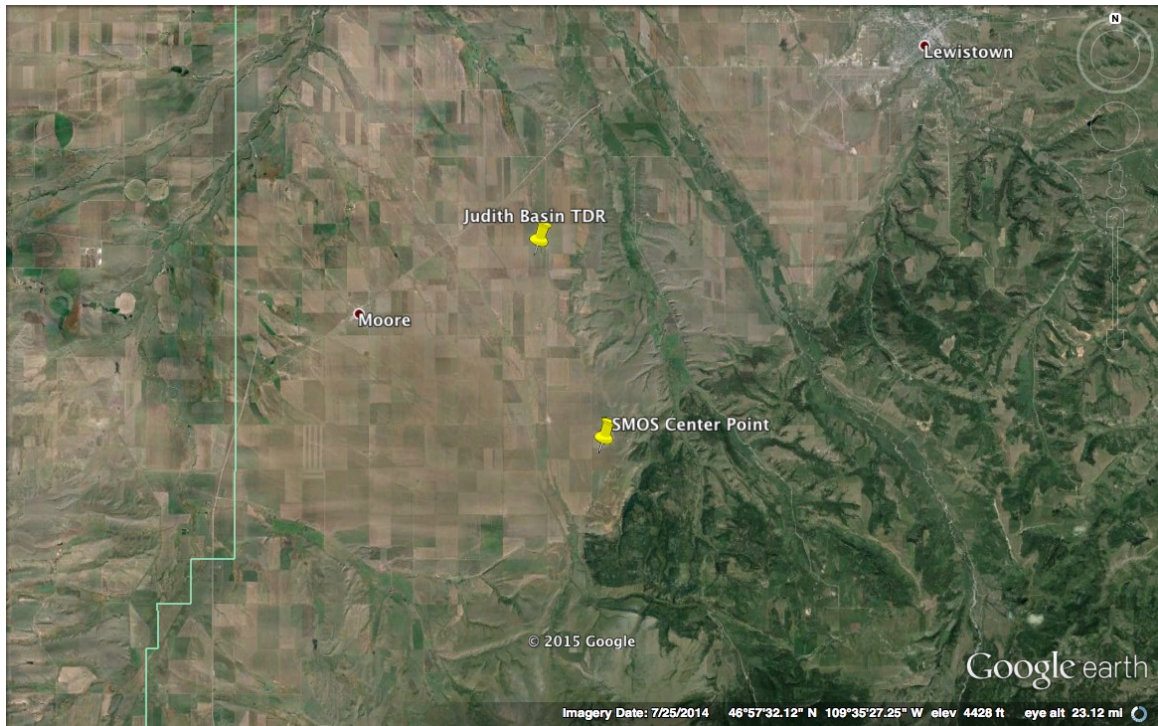


Figure 4: The locations of the Judith Basin time domain reflectometry (TDR) observations and Judith Basin SMOS Center point.



Figure 5: The locations of the Fort Peck COSMOS observations and the corresponding SMOS center point.

References

- Ford TW, Harris E, Quiring SM (2013) Estimating root zone soil moisture using near-surface observations from SMOS. *Hydrol Earth Syst Sci Discuss* 10:8325–8364. doi: 10.5194/hessd-10-8325-2013
- Katul GG, Porporato A, Daly E, et al. (2007) On the spectrum of soil moisture in a shallow-rooted uniform pine forest: from hourly to inter-annual time scales. *Water Resour Res* 43:doi:10.1029/2006WR005356.
- Rodriguez-Iturbe I, Porporato A (2004) *Ecohydrology of water controlled ecosystems: plants and soil moisture dynamics*. Cambridge University Press, Cambridge, UK
- Sheffield J, Goteti G, Wood EF (2006) Development of a 50-year high-resolution global dataset of meteorological forcings for land surface modeling. *J Clim* 19:3088–3111.
- Stoy PC (2013) The climate record of Montana over the past half-century. Consequences for water resources and opportunities for teaching practitioners how to study the whole bowl of cherries. *Mont. Sect. Am. Water Resour. Assoc. 2013 Conf.*

Wallace JS, Batchelor CH (1997) Managing water resources for crop production. *Philos Trans R Soc London Ser B Biol Sci* 352:937–947. doi: 10.1098/rstb.1997.0073

Zreda M, Desilets D, Ferré TPA, Scott RL (2008) Measuring soil moisture content non-invasively at intermediate spatial scale using cosmic-ray neutrons. *Geophys Res Lett* 35:L21402. doi: 10.1029/2008GL035655

Contaminants monitoring and natal dispersal of ospreys along the Yellowstone River

Basic Information

Title:	Contaminants monitoring and natal dispersal of ospreys along the Yellowstone River
Project Number:	2014MT285B
Start Date:	3/1/2014
End Date:	2/28/2015
Funding Source:	104B
Congressional District:	MT 1
Research Category:	Water Quality
Focus Category:	Toxic Substances, None, None
Descriptors:	None
Principal Investigators:	Kayhan Ostovar

Publications

There are no publications.



Final Report to USGS Water Center SEED Grant – MSU Bozeman

Project Title: **CONTAMINANTS MONITORING AND NATAL DISPERSAL OF OSPREYS ALONG THE YELLOWSTONE RIVER, MT**

The primary goal of this project was to evaluate the health of the Yellowstone River ecosystem by monitoring a sentinel species, the osprey for heavy metal contaminants. We had a very successful 2014 and received nice coverage by several local papers:

- 1) http://billingsgazette.com/news/local/nesting-instincts-osprey-chicks-examined-as-part-of-research-program/article_e87c16e9-fb05-59f5-8a39-200306cc3f91.html This story mentions the USGS Water Center grant.
- 2) See attached copy of another story that featured one of the students and which also mentions the Water Center grant.

Matching funds for the USGS Water Center SEED grant were received from the Cinnabar Foundation, RMC's SEED Program, the Yellowstone River Research Center, and the Royal Bank of Canada Blue Water Project.

In 2014 the osprey project grew substantially. In May we held a training session at Rocky Mountain College for volunteers and had a large team of citizen scientists sign up to help observe behavior at 50 occupied nests. We banded 59 chicks with USGS bands as well as uniquely coded alphanumeric color bands. These color bands will allow for the individual identification of ospreys in our area in the future. This year some of the young birds were sighted in the Gulf of Mexico. All band numbers and fledgling success rates were submitted to the Montana Natural Heritage Center and Montana Fish Wildlife and Parks. Blood analysis work by University of Montana was recently completed on 27 blood samples from 2014.

Two undergraduate students at RMC conducted additional independent research projects related to osprey and the heavy metal study. The first study (**Osprey foraging behavior and fledgling success along the Yellowstone River, MT**) continued examining foraging behavior and reproductive success of osprey along the Yellowstone River. Starting in 2013 long-term behavioral observations were conducted on 20 nests along the Yellowstone River and detailed prey deliveries were recorded. Another student looked at blood chemistry panels (**Baseline hematological values for osprey nestlings on the Yellowstone River, MT**)

sampled from chicks <http://yellowstoneriver.weebly.com/2014-reports.html>
Both of these efforts may help us better understand heavy metal contaminant patterns observed in the osprey blood from the three year study.

Hands-on undergraduate research provided unique opportunities for students to carry out graduate level work and share this information with the community, land managers and conservationists. During the last three years our field work with four undergraduate students allowed them to receive training in how to properly handle birds, draw blood and band them safely. A paper was recently published in the Canadian Field Naturalist with Renee Seacor (undergraduate student) as senior author.

http://yellowstoneriver.weebly.com/uploads/1/0/7/6/10768367/seacor_ostovar_restani_2014_osprey.pdf

This three year heavy metal project wrapped up in 2014 and the data is now being analyzed. We have a co-authorship agreement in place with another collaborator on the project for all four students to be recognized in a final paper with an undergraduate student listed as the primary author. Analysis of the heavy metal blood results is occurring now with a proposed completion of the paper by the end of the summer. We hope to present these results at regional conferences such as the MT Chapter of the Society for Conservation Biology and the Wildlife Society Montana Chapter annual meetings next year. Two undergraduate students presented their research talks at the annual YRRC forum and RMC research event in 2014 and 2015.

In 2015 we plan to transition to a spiny softshell and snapping turtle study on both the Yellowstone and Musselshell Rivers. While ospreys are good indicators of environmental contaminants, turtles may prove even better since they do not migrate and are also piscivorous. In addition both these native Montana turtles are listed by Montana Fish Wildlife and Parks as Species of Concern. There is a unique opportunity to document declines in heavy metal contaminants in wildlife related to the 2015 closure of the Corette coal-powered electric plant in Billings.

Finally, we continued to help raise awareness about pollution issues on the Yellowstone River with the results from this study and engage the public in our annual river cleanup float. This year we had 75 people on the river plus another 25 on shore-based teams. The group removed over 7,000 lbs of metal which all went to a recycling yard plus piles of tires and other trash.

Two good pictures from the 2014 field season.



Ranch kids holding fledgling osprey.

Thank you for the opportunity,

Associate Professor Kayhan Ostovar

A handwritten signature in black ink, appearing to read 'Kayhan Ostovar', written in a cursive style.

Student Fellowship: The Impact of Irrigation on the Hydrologic Cycle under Low Water Availability

Basic Information

Title:	Student Fellowship: The Impact of Irrigation on the Hydrologic Cycle under Low Water Availability
Project Number:	2014MT286B
Start Date:	3/1/2014
End Date:	2/28/2015
Funding Source:	104B
Congressional District:	MT 1
Research Category:	Climate and Hydrologic Processes
Focus Category:	Irrigation, None, None
Descriptors:	None
Principal Investigators:	Douglas Brugger

Publications

There are no publications.

Doug Brugger, PhD Student in Geosciences at the University of Montana
Advisor – Marco Maneta
MT Water Center Final Report – Spring 2015

RESEARCH SUMMARY

The goal of my research has been to build a parsimonious yet comprehensive model of how agriculture interacts with water resources so that the long-term behavior and stability of the coupled system can be better understood. My advisor and I have focused on the conversion of agricultural land to non-agricultural use. In most Western Montana counties, total agricultural land is steadily decreasing due to A) the tenuous economic return of agricultural activities and B) growing urban centers increasing the demand for non-agricultural land use. We are investigating 1) the relative impacts of climate and economics on the conversion of agricultural land and 2) the long-term dynamics of agricultural land and implications for the hydrologic cycle. We have built a computational model to address these questions and are using the Bitterroot River Watershed and the nearly contiguous Ravalli County as a case study.

Our model couples hydrology and agricultural economics based on the schematic in Figure 1. The hydrologic model is driven by precipitation and potential evapotranspiration (PET) products from the MOD16 program. The model divides the Bitterroot River watershed into compartments based on land cover type and is run at an annual timestep. The model was calibrated to USGS-gaged streamflow and actual ET from the MOD16 program (Figure 2). Soil moisture from the hydrologic model is used to calculate yield with a power law relationship that was calibrated to data from the US Department of Agriculture's National Agricultural Statistics Service (NASS), see Figure 3. These yields are used by an economic model to calculate revenue; the economic model accounts for crop prices, production costs, and the market value of the agricultural land (determined using the Montana Cadastral database) to calculate the fraction of agricultural land that is sold for non-agricultural use. The economic model also accounts for grazing land and livestock, though these are not explicitly coupled to the hydrologic model.

The coarse resolution of our model means that the model can be parameterized with readily available economic data from NASS. However, representing agricultural land with one “average” farm for a county would be too coarse. Smaller and larger farms operate differently, and smaller farms are typically closer to urbanized areas and have higher market value. We have used a novel approach to account for this by fitting multiple Gaussian distributions to the distribution of agricultural parcels (Figure 5). This allows for independent treatment of different farm size “groups” represented statistically by separate Gaussian distributions. The distributions are conducive to quick calculations with robust statistical interpretations.

The model has been able to reproduce the observed behavior of agricultural land in Ravalli County fairly well. The overall trends are captured, as well as some of the fluctuations that are superimposed on this trend. These fluctuations are caused by variability in economics and, in the case of rainfed agriculture, variations in climate, which can cause years with poor yield and relatively high conversion rates of agricultural land.

The model is performing well, but there are challenges due to poor accuracy of economic data, which is derived from surveys. For example, because rainfed agriculture is a small portion of total agriculture in Ravalli County the survey results aren't as accurate as with irrigated or grazing land. The data shows rainfed agricultural land area increasing sporadically over the study period, which is likely not the case, at least to the degree suggested by the data. Even with this challenge, the model gives insight into the sensitivity and stability of the system. We can use the model to ask questions such as "how much will irrigation use of water decrease if economic conditions are steady, compared to an increase in land value caused by urban growth?" or "how will the rate of land conversion be affected by a shift in precipitation from snow to rain?" We are in the process of investigating these questions and we plan on submitting a manuscript on the model by this fall.

PROFESSIONAL DEVELOPMENT & OUTREACH

- Presentations

- UM's Graduate Student Research Conference, 2014 (poster) and 2015 (presentation)
- Montana Space Grant Consortium Conference, 2014 (poster)

- I've given demonstrations at SpectrUM, an interactive science museum in Missoula aimed at primary school children. I use the Geoscience department's groundwater models that resemble an ant farm. There are multiple "wells" in the model where the students can inject dye to see the path of groundwater flow. The simplified model gets them thinking about real-world aquifer contamination, which often brings as many questions from the parents as from the students.

- Water sciences are inherently interdisciplinary and there is an undeniable need for productive collaborative projects. In order to start interdisciplinary thinking as a graduate student I've volunteered with a new group on our campus, the Interdisciplinary Collaborative Network. This is a grassroots organization that facilitates collaboration between graduate students. We started the "Collaboration Challenge" program in Fall 2014, which provides funding and awards for graduate students who initiate interdisciplinary collaboration as part of their graduate research.

FIGURES

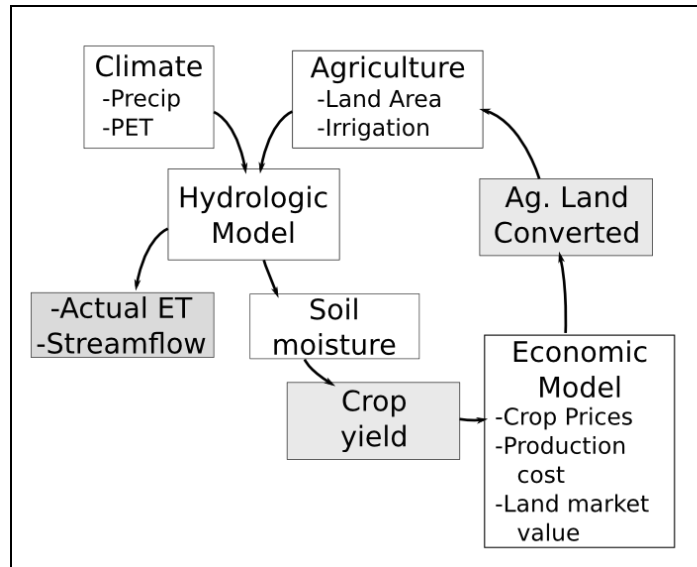


Figure 1 – Coupled model schematic. Boxes with shaded background are calibration targets.

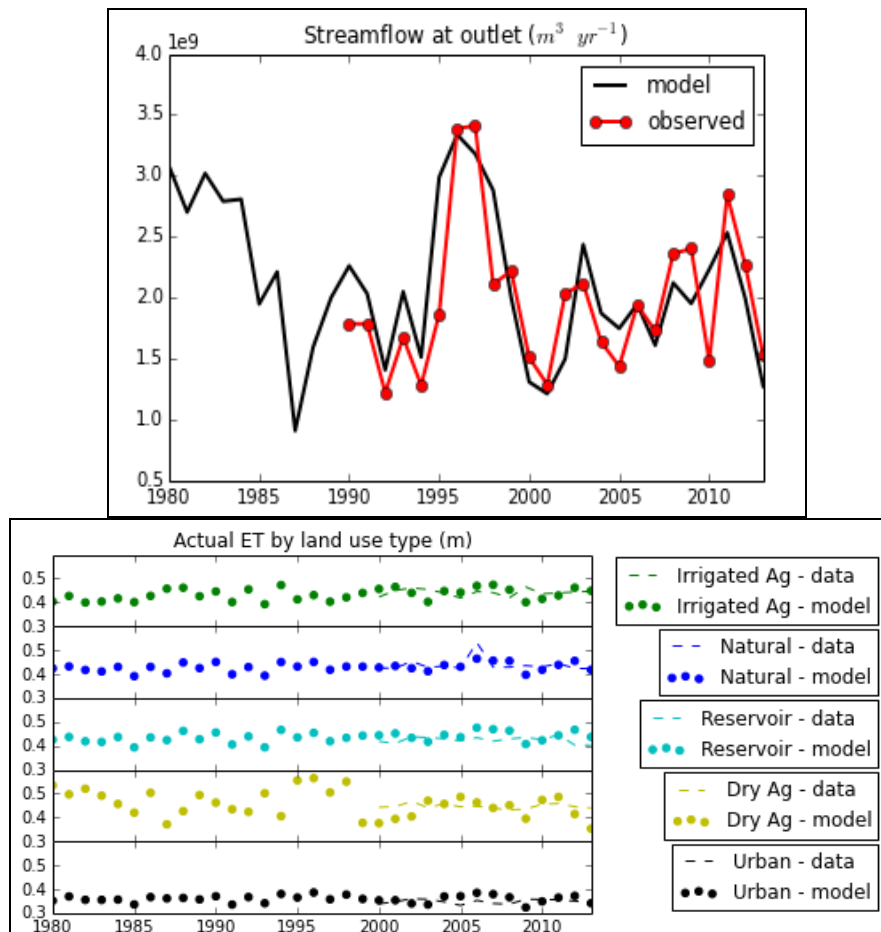


Figure 2 – Hydrologic calibration results, streamflow for the Bitterroot River near Missoula (top) and evapotranspiration from the multiple land cover types (bottom)

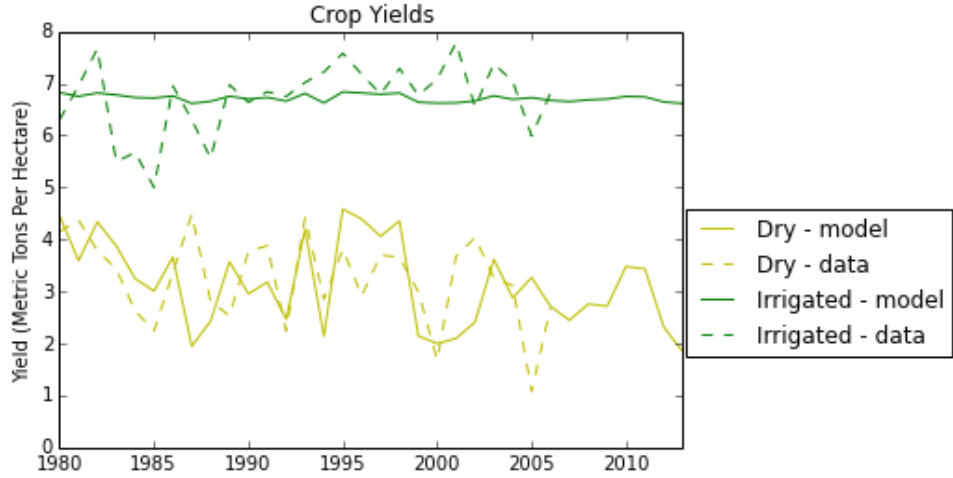


Figure 3 – Yield Calibration Results..

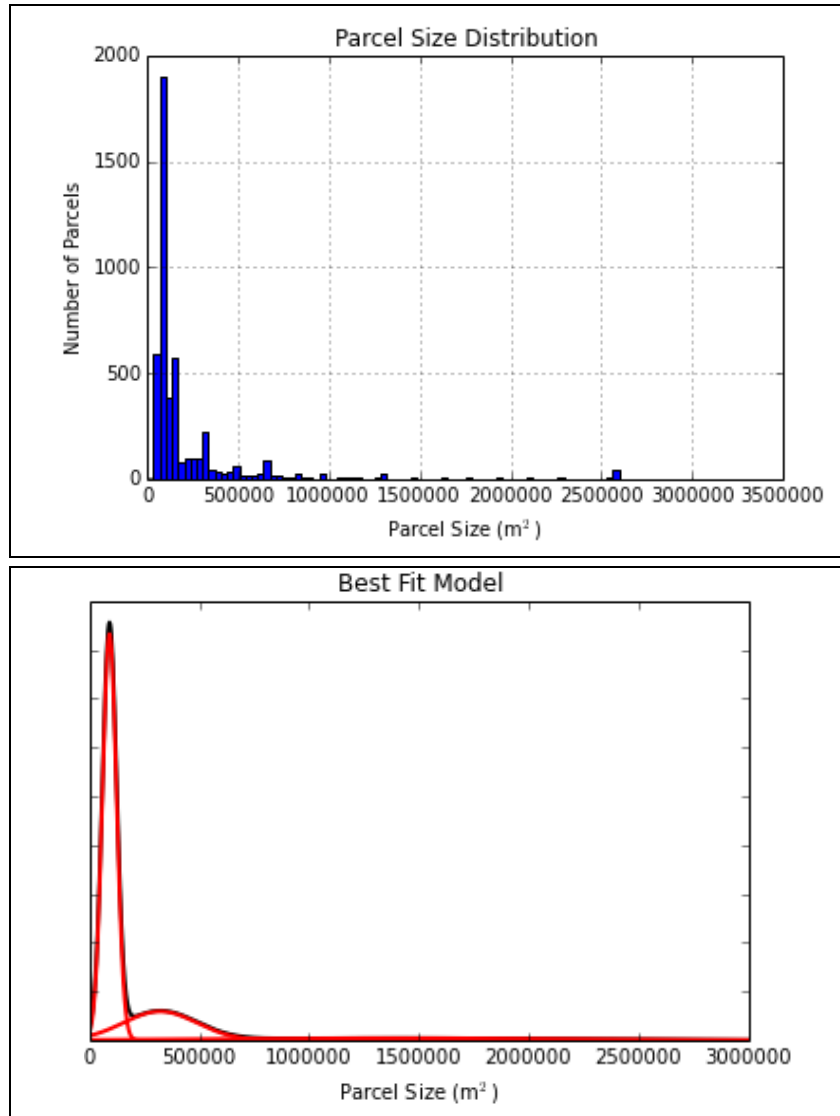


Figure 4 –Gaussian Distributions fit to the distribution of parcel sizes in Ravalli County

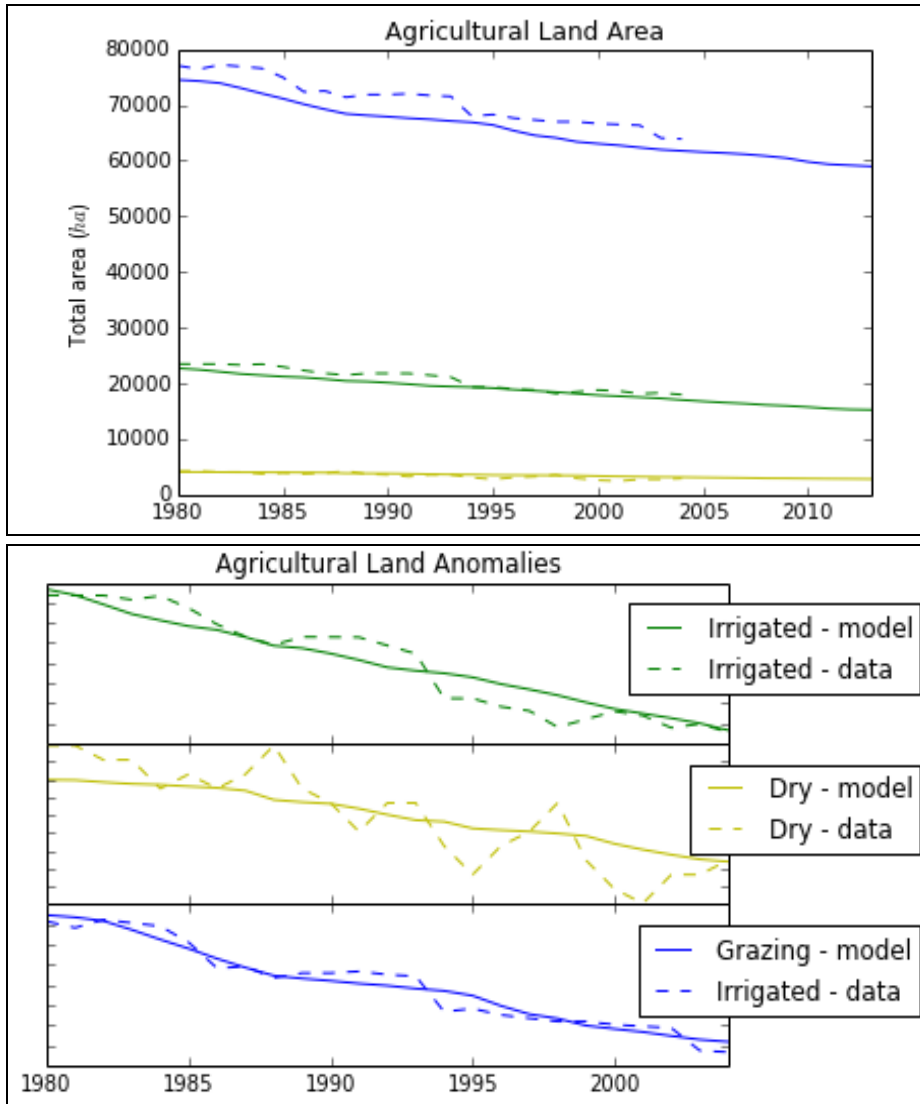


Figure 5 – Agricultural land conversion results, as total area (top) and anomaly (bottom).

Student Fellowship: Thresholds of Hydrologic Connectivity: Shallow Water Table Development at the Hillslope Scale

Basic Information

Title:	Student Fellowship: Thresholds of Hydrologic Connectivity: Shallow Water Table Development at the Hillslope Scale
Project Number:	2014MT287B
Start Date:	3/1/2014
End Date:	2/28/2015
Funding Source:	104B
Congressional District:	MT 1
Research Category:	Ground-water Flow and Transport
Focus Category:	Groundwater, None, None
Descriptors:	None
Principal Investigators:	Emily Clark

Publications

There are no publications.

Shallow subsurface stormflow through the soil zone is often the dominant mode of runoff contributions in mountainous terrain, but the dynamics of hillslope hydrology are highly variable and complex. The effects of landscape organization on shallow subsurface flow, water table development, and runoff source areas are poorly understood. Distinguishing watershed characteristics that influence the temporal and spatial response of shallow subsurface flow within hillslopes is requisite for predicting streamflow quantity, quality, and timing. We ask the question: at what scale do characteristics of surface topography best enhance predictions of shallow groundwater response and contributions to streams? To evaluate this question we analyzed the ability of local and non-local (upslope) terrain attributes to predict shallow groundwater dynamics in 24 wells across 3 hillslopes of low-permeability soils but distinct shape and size in a 630 hectare watershed. The results presented in this study strongly suggest that surface terrain attributes can predict temporal and spatial patterns of shallow groundwater. Our study corroborates prior findings of predictive power in upslope accumulated area (UAA) and local slope, but emphasize the importance of considering the two variables independently, as each has unique forecasting capabilities. To accurately estimate shallow groundwater behavior in hillslopes, one must assess topographic architecture at the macro-scale (the entire spatial extent of hillslope drainage area) as well as the localized-scale (the local slope at a monitoring site). Evaluation of UAA and local slope individually indicates that as upslope area increases and slope decreases, there is a higher probability of a greater magnitude in water table response. UAA was an essential catchment trait to gauge the magnitude of hillslope runoff contributions to streamflow.

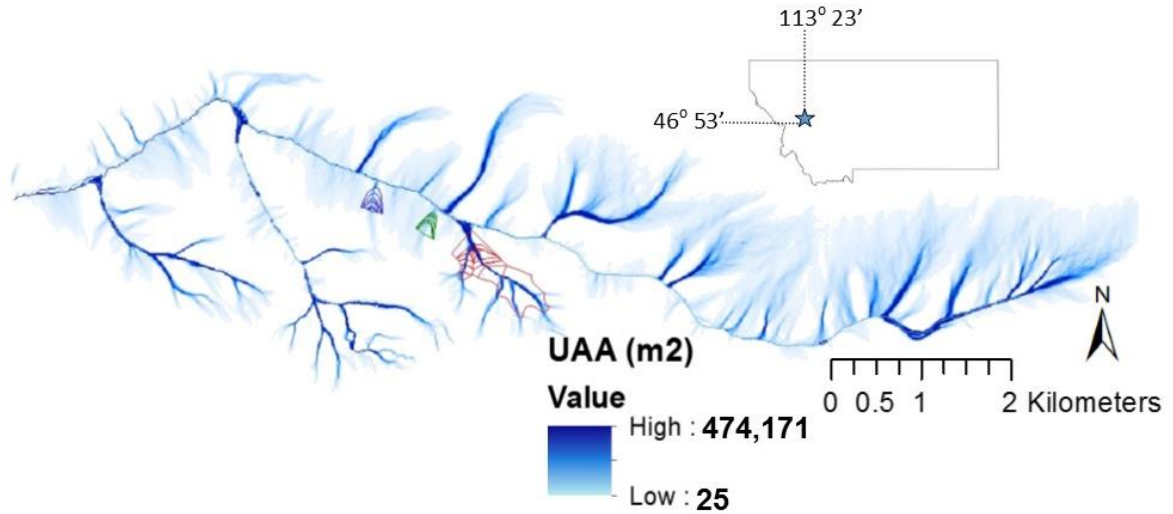


Figure 1. Cap Wallace study catchment in Montana, USA. Watershed map illustrates distribution of upslope accumulated area (UAA) and flow boundary delineation for three study hillslopes: large (red), medium (blue), and small (green).

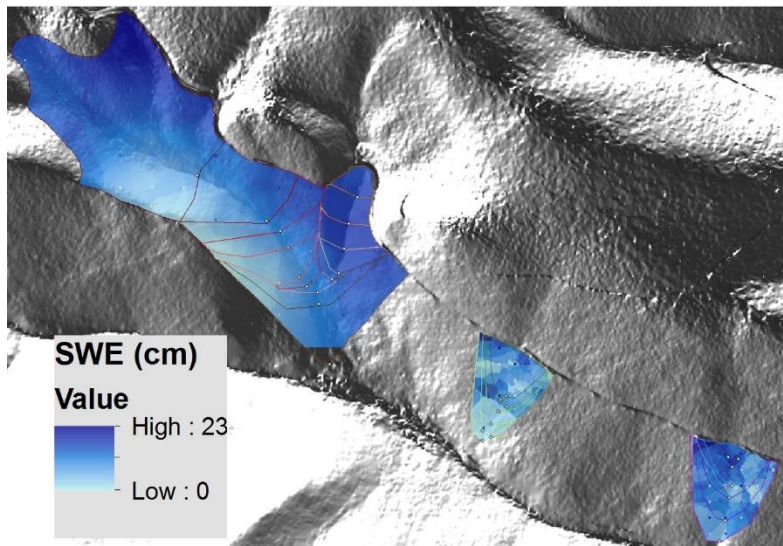


Figure 2. Snow water equivalent (SWE) distributions across the study slopes measured on March 21st and 23rd of 2014. Variation in SWE values were interpolated with a bilinear kriging method.

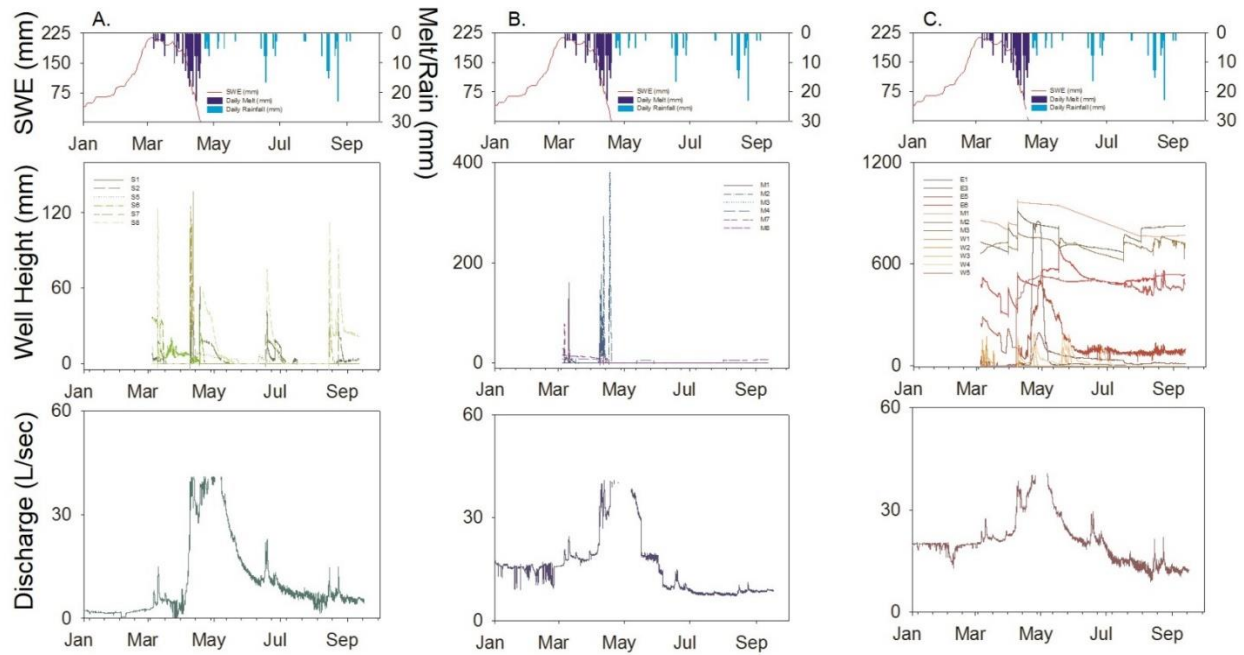


Figure 3. Time series of hydrologic conditions across 3 study slopes: small (A), medium (B), large (C). Snow accumulation, snowmelt and rain inputs, well responses per hillslope, and hydrographs of streamflow below each contributing study slope. The maximum response in hillslopes and streams was during the snowmelt pulse. Water table responses to rain events occurred in the small and large hillslopes. Antecedent moisture in the medium slope was too low to elicit substantial wet-up of wells during summer and fall rain events. Note the scale differences for well height between our 3 slopes.

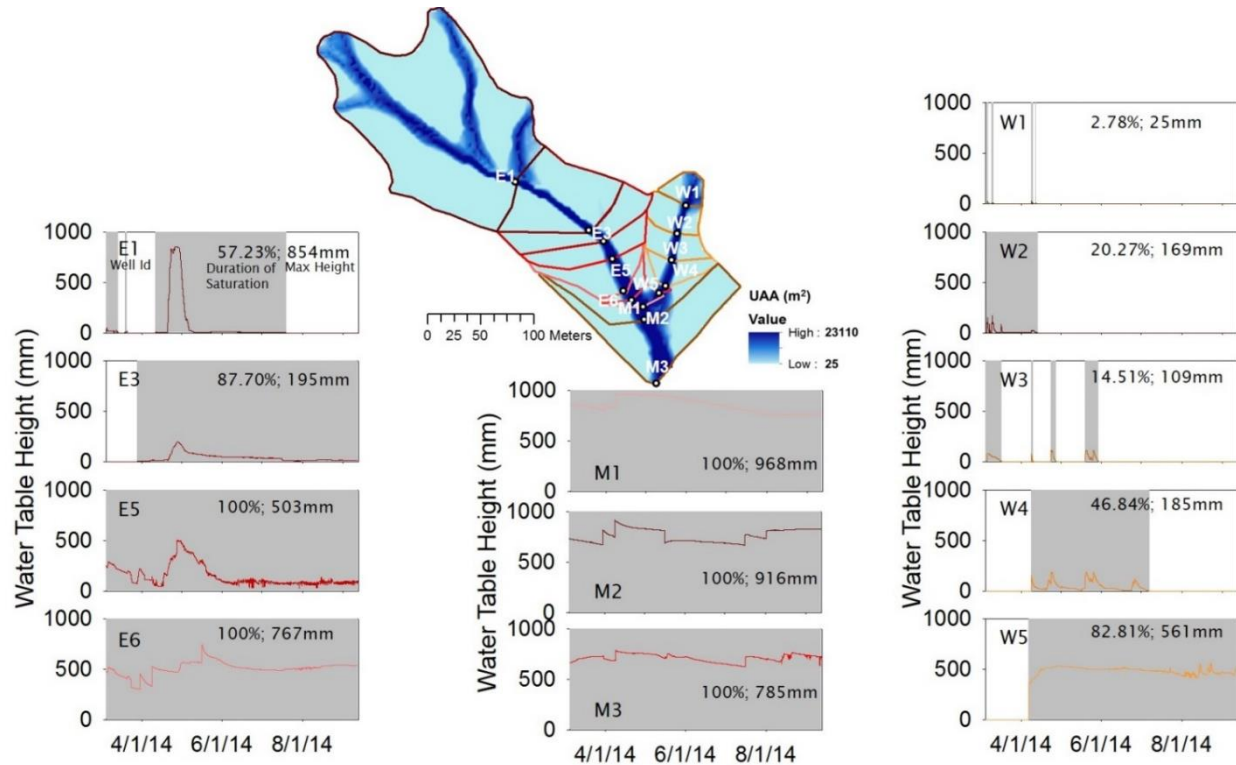


Figure 4. Groundwater well dynamics across the large study slope. Grey bars highlight time period of saturation at each well. Each graph lists the duration of saturation and maximum water table height. Lines on the map represent the LCA to each recording well. The UAA map demonstrates variability in topographically defined flow accumulation. Groundwater wells in areas of higher area accumulation remained saturated for greater periods of time. Well locations span a range of landscape positions capturing characteristic behavior of transient shallow groundwater response on hillslopes (E1, E3, W1, W2, W3), more sustained groundwater response on the toe slopes (E5, W4, W5), and persistent saturation in the valley bottom (E6, M1, M2, M3).

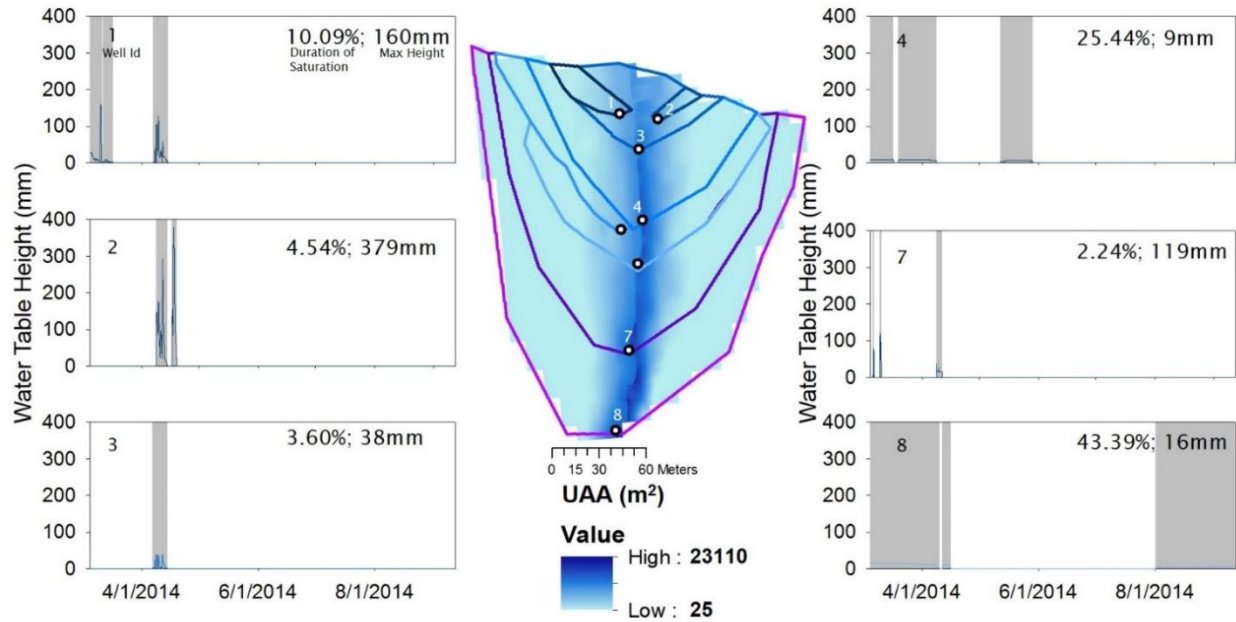


Figure 5. Groundwater well dynamics across the medium study slope. Grey bars highlight time period of saturation at each well. Each graph lists the duration of saturation and maximum water table height. Lines on the map represent the LCA to each recording well. The UAA map demonstrates variability in topographically defined flow accumulation. Groundwater wells in areas of higher area accumulation remained saturated for greater periods of time.

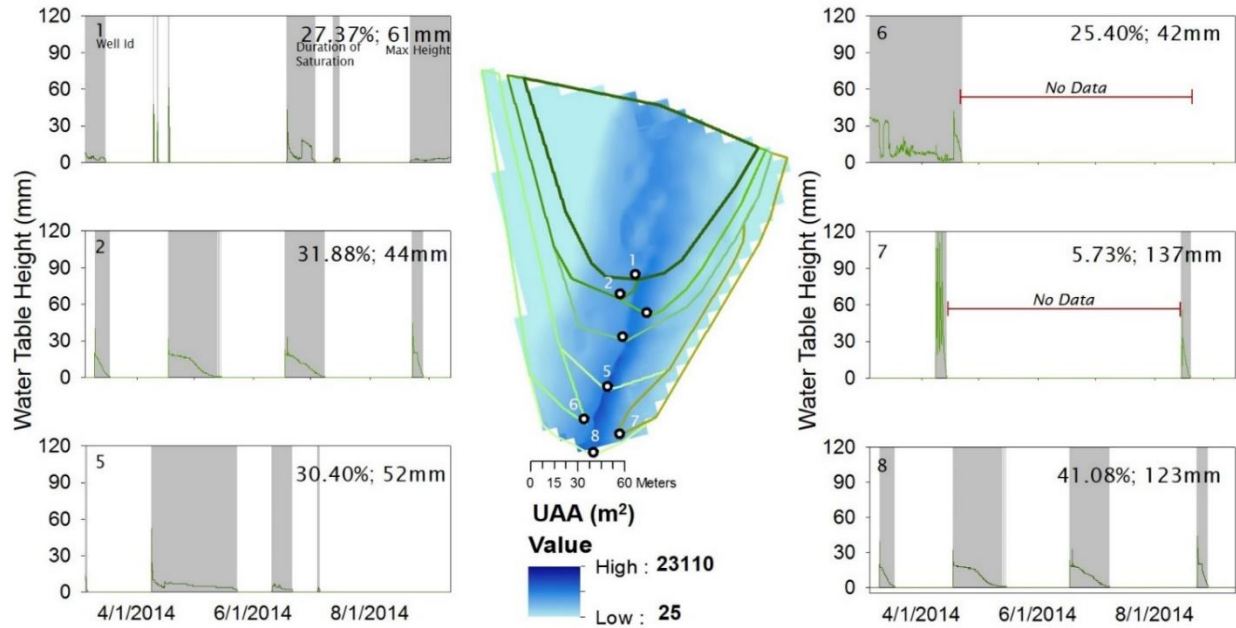


Figure 6. Groundwater well dynamics across the small study slope. Grey bars highlight time period of saturation at each well. Each graph lists the duration of saturation and maximum water table height. Lines on the map represent the LCA to each recording well. The UAA map demonstrates variability in topographically defined flow accumulation. Groundwater wells in areas of higher area accumulation remained saturated for greater periods of time.

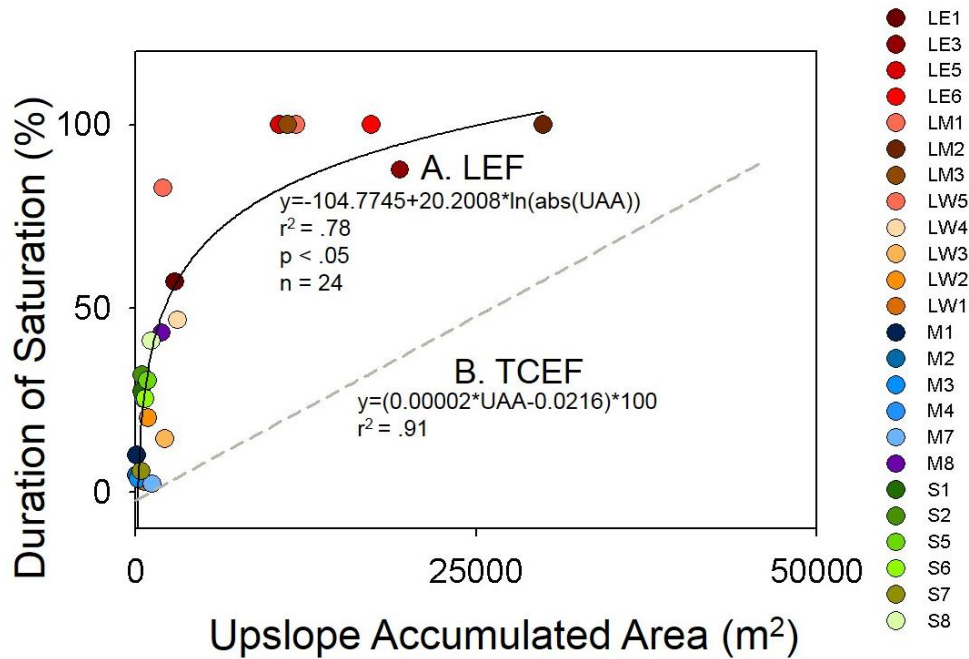


Figure 7. The duration of saturation at each study well as a logarithmic function of UAA. In the Lubrecht Experimental Forest (LEF), continuous saturation is probable near 10,000 m² of accumulated area (A). UAA and duration of saturation relationship findings are corroborated by research in Tenderfoot Creek Experimental Forest (TCEF), but demonstrate differences among sites (B). Coarser soil in TCEF likely require a greater accumulation of area for similar saturation response relative to the low permeable soils of LEF.

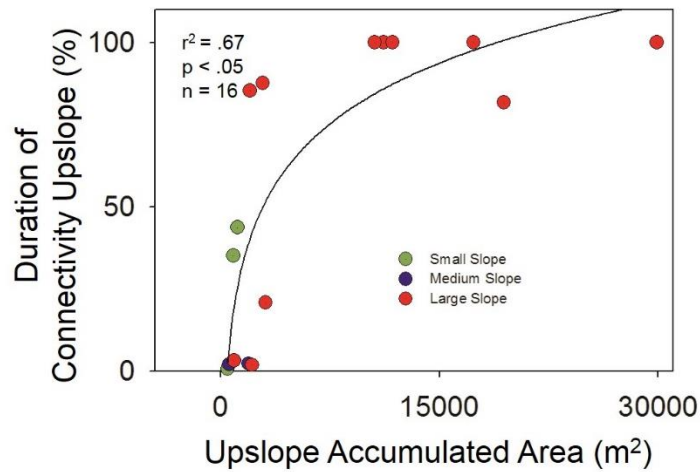


Figure 8. Proportion of time that saturation existed between consecutive wells as a function of UAA. The large study slope exhibits greater temporal and spatial extents of hydrologic connectivity relative to the two smaller slopes of lesser convergence.

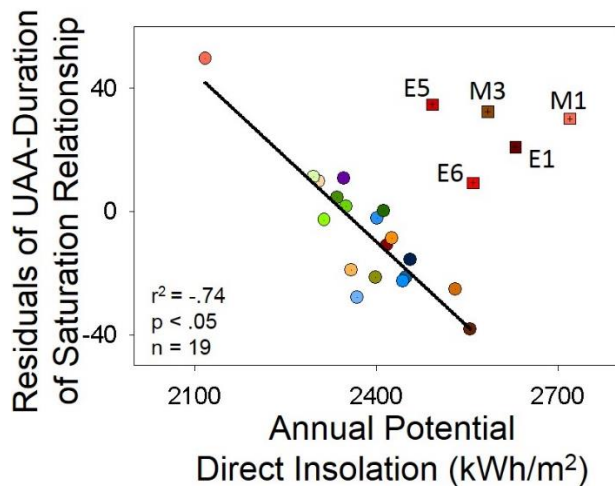


Figure 9. Residual values from the UAA and duration of saturation relationship plotted as a function of total annual potential direct solar insolation. Increased potential insolation was associated with less than expected saturation across the study hillslopes. This suggests that potential insolation contributed to increased ablation of snowpack, rapid snowmelt, and reduced

duration of saturation. Riparian and toe slope wells with persistent saturation exhibited unique behavior relative to the hillslope wells and were separated from the linear regression model.

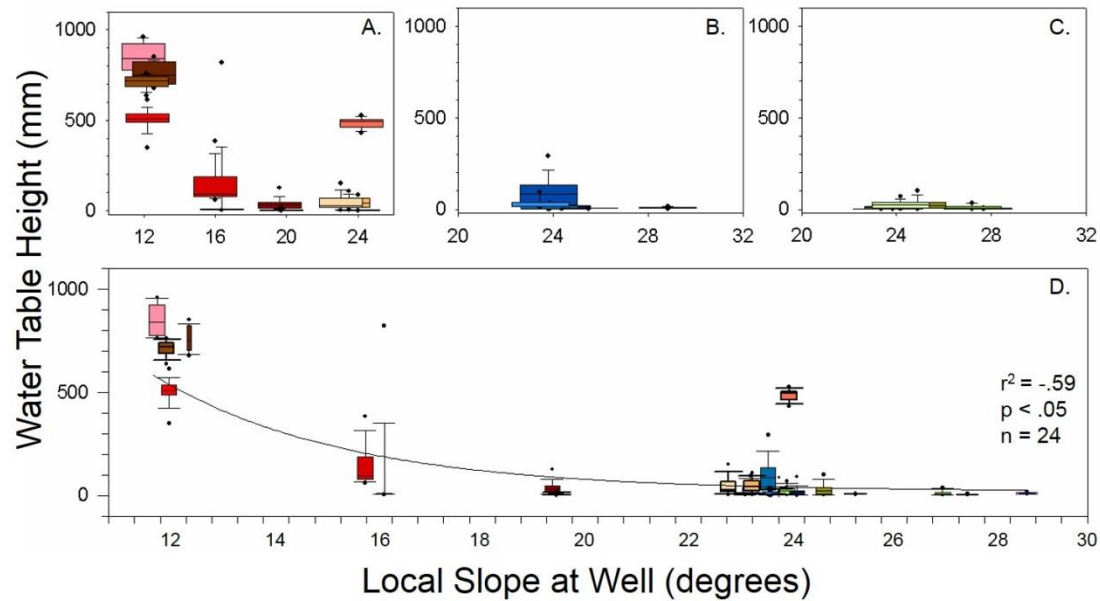


Figure 10. Box plots of each water table time series as a function of local slope at the well. Instrumentation across the large slope encompasses diverse landscape positions and slope gradients, and thus, results in the greatest observed variance in water table response (A). The medium and small slope wells were sited along similar slope gradients, but the small slope's response was consistent (C), whereas the medium slope was flashy (B). Across the three study sites, increasing slope generally resulted in decreasing water table magnitudes.

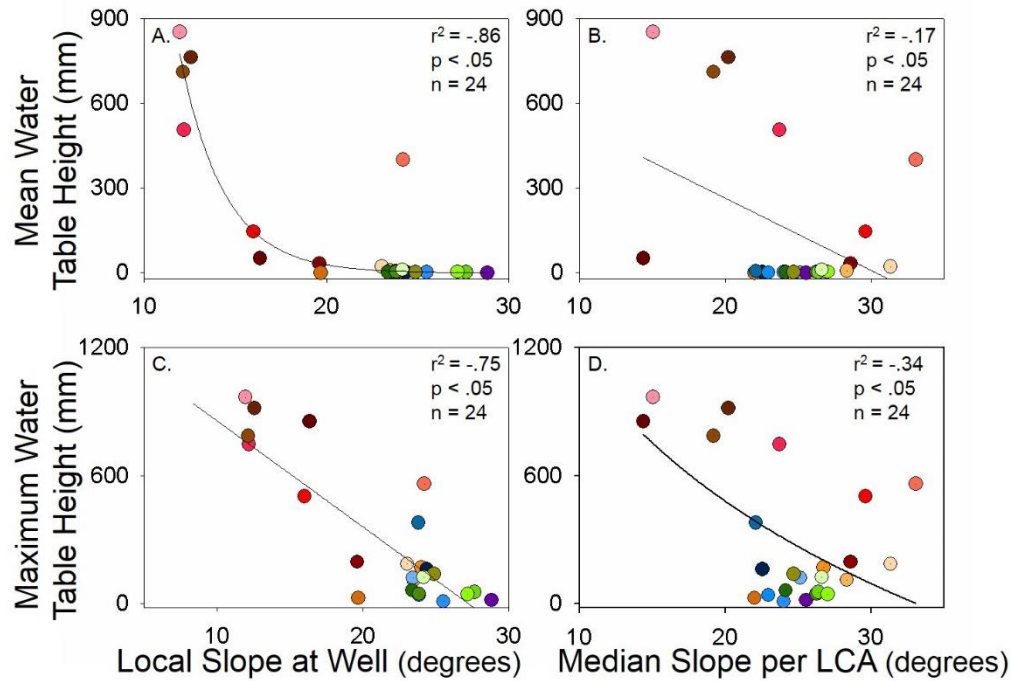


Figure 11. Mean water table height as a function of local slope at the well site 5m grid cell (A) and the median slope of the lateral contributing area (LCA) per well (B). Maximum water table height with respect to the local slope at the well 5m grid cell (C) and the median slope per LCA (D). Local slope is a dominant modulator of groundwater dynamics. Contributions of soil water depend on upslope controls of area, but the potential magnitude and average behavior of water table response is highly correlated to slope immediately surrounding the measurement point.

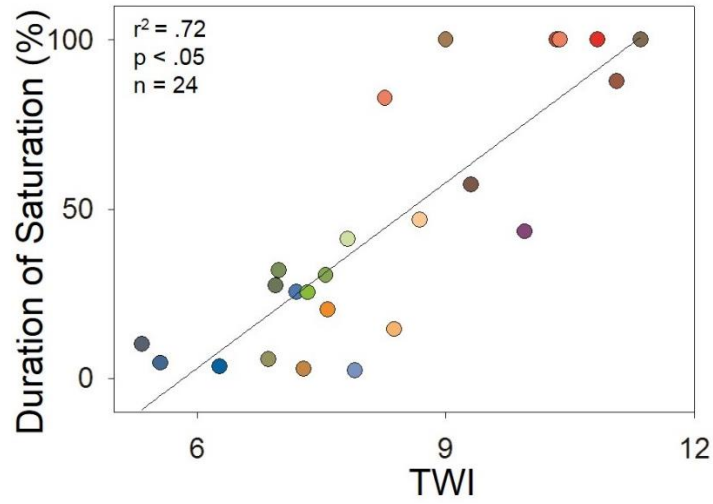


Figure 12. Linear regression of the Topographic Wetness Index (TWI) against duration of water table presence. Utilizing upslope (UAA) and local (slope) metrics in a compound index of TWI sufficiently explains variance in water table temporal response.

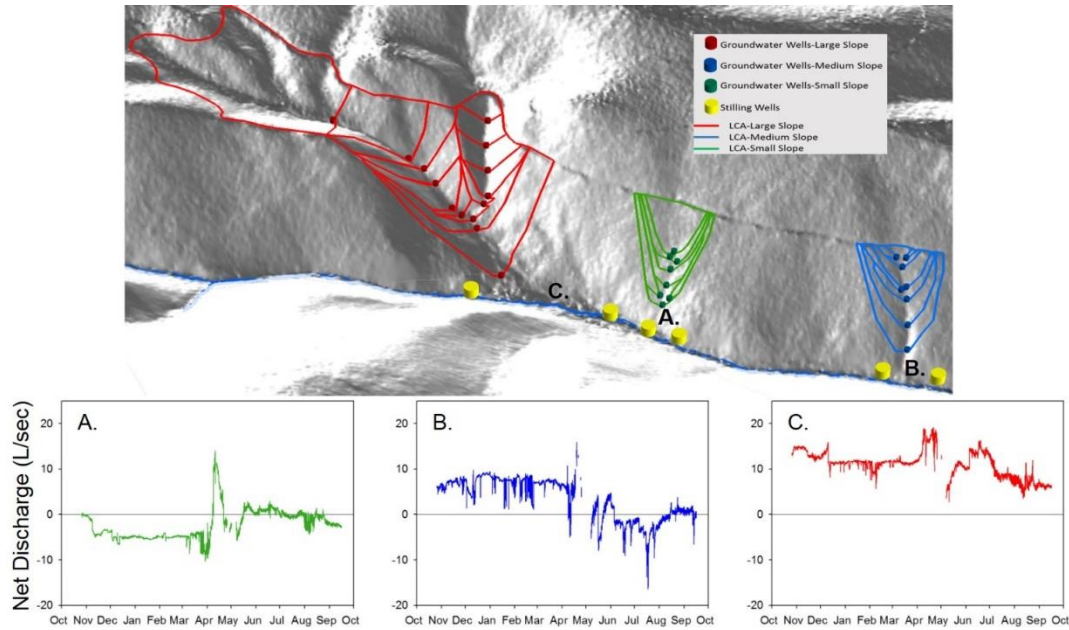


Figure 13. Map of groundwater and stilling well instrumentation and LCAs per well. Graphical comparison of net discharge from the lateral contributing area associated with each study hillslope. The greatest net discharge was observed at the stream reach along the large slope (B). The smallest hillslope stream reach resulted in the least amount of discharge gains (C). The medium slope stream reach gained net discharge until snowmelt recession (D).

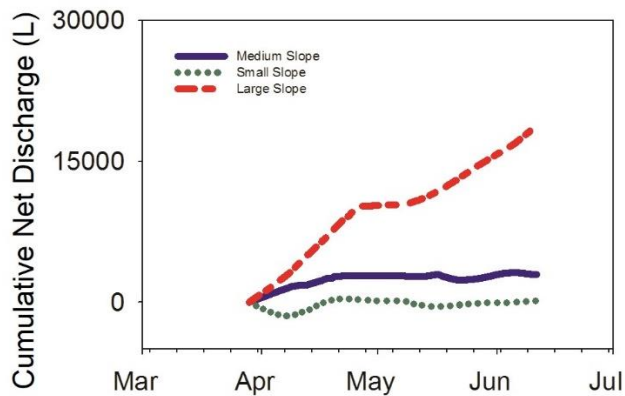


Figure 14. Time series comparing cumulative net discharge across study slope stream reaches during snowmelt (3/28/14-6/11/14). The size of slope contributing area was comparable to values of net gains in adjacent stream reach.



To gauge the magnitude and duration of shallow water table development, perforated pipes were driven to the soil-bedrock interface. Emily is pictured sealing the surface of the welling with clay.



Capacitance rods were suspended in hillslope wells to record the height and duration of the watertable. These instruments allowed us to compare shallow subsurface flow within a single hillslope and across the three sites.



Dilution gauging was performed on Cap Wallace Creek six times across variable flow states in 2014. The difference between discharge measurements upstream and downstream of each hillslope transect was used to quantify the net change in flow that may be linked to contributions of water from the study hillslopes.



We collected measurements of snow water equivalent at the time of peak snow pack to quantify the potential spatial variability of snow water inputs across our three study slopes.

Student Fellowship: Seasonal Timing of Evapotranspiration and the Effect on Soil Moisture and Water Availability for Groundwater Recharge with Different Crop Rotation Practices

Basic Information

Title:	Student Fellowship: Seasonal Timing of Evapotranspiration and the Effect on Soil Moisture and Water Availability for Groundwater Recharge with Different Crop Rotation Practices
Project Number:	2014MT288B
Start Date:	3/1/2014
End Date:	2/28/2015
Funding Source:	104B
Congressional District:	MT 1
Research Category:	Ground-water Flow and Transport
Focus Category:	Groundwater, Hydrology, None
Descriptors:	None
Principal Investigators:	Elizabeth Harris

Publications

There are no publications.

Montana Water Center Student Research Fellowship

Final Report

by

Elizabeth S.K. Harris

List of objectives stated in the proposal:

Objective 1: To quantify water storage in a fallow field rotation.

One (of many) reasons for fallow field rotation is the notion that soil water is replenished by limiting plant growth. The purpose of this objective is to determine how much water is stored due to the fallow field rotation. I will quantify the impacts of fallow on water storage by comparing soil moisture and evapotranspiration measurements from a fallow field to soil moisture and evapotranspiration measurements from a spring wheat field during the course of the growing season.

Objective 2: To measure the evapotranspiration occurrence throughout the year.

We will better understand fluctuations in evapotranspiration due to seasonal changes in climate and crop management for increased knowledge in how energy available for potential evapotranspiration is related to actual evapotranspiration throughout the year.

Objective 3: Determine water availability for groundwater recharge.

By measuring precipitation, soil moisture, and evapotranspiration we can determine water inputs, outputs, and the movement of water in the soil column.

Introduction:

Wheat supplies 9% of the world's food (Anthoni et al., 2004) and is the principal crop in the dryland agricultural systems of Montana. Uniquely for the Montana dryland-cropping ecosystem, wheat-fallow rotations often outperform other rotations on an economic basis in drier parts of the state (Aase and Schaefer, 1996), leaving upwards of 40% of the state's largest wheat growing region, the Golden Triangle, in fallow during a typical growing season. It is important that we are able to quantify water use in wheat for hydrologic planning and amid growing concerns that global wheat production is in decline as a response to rising temperatures and thereby evaporative demand (Asseng et al., 2014; Figure 1).

The difference in evapotranspiration from wheat and fallow fields is rarely measured, nor is the surface-atmosphere exchange of sensible heat which has important consequences for atmospheric boundary layer height and the probability of convective precipitation (Luyseart et al., 2014; Juang et al., 2007a,b). Reducing fallow may have positive benefits for regional hydroclimatology. Gameda et al. (2007) found that a reduction in summer fallow from 10 Mha to 3.5 Mha in the Canadian Prairie Provinces was related to an increase in summertime precipitation on the order of 10 mm/decade, a decrease in maximum temperature and diurnal temperature range of 1.7 °C/decade and 1.1 °C/decade, respectively, and a -6 W m^{-2} summertime radiative forcing due largely to an increase in cloudiness. Such a cooling effect of widespread fallow reduction may help avoid the detrimental impacts of heat on the wheat crop and place Montana producers at a competitive advantage against global wheat producers who are experiencing a decline in wheat production due to increasing global temperatures (Asseng et al., 2014).

Materials and Methods:

Site Information The study sites are located in the Judith River basin near Moore, Montana (Figure 2). On May 5, 2013 spring wheat was planted in a field where a flux tower – hereafter the ‘wheat tower’ - was installed at $46^{\circ} 59' 41.100''$ N, $109^{\circ} 36' 49.500''$ W. The wheat tower was removed in September 2014 after the harvest on August 18, 2014. A second tower - hereafter the ‘fallow tower’ - was installed at $46^{\circ} 59' 44.800''$ N, $109^{\circ} 37' 46.300''$ W in a no-till fallow field in October 2013, 1.2 km from the wheat field tower, and removed about the same time as the wheat tower.

Turbulent Flux Measurements The surface-atmosphere flux of latent heat (LE) was made using the eddy covariance technique. This involved the coupling of a CSAT-3 sonic anemometer (Campbell Scientific Inc., Logan, UT) with enclosed path LI-7200 CO₂/H₂O infrared gas analyzers (LiCor, Lincoln, NE) installed 1.8 meters above the ground surface in the case of both towers. Sensible heat exchange (H) was measured using a sonic anemometer. Data were recorded at 10 Hz on a CR3000 data logger (Campbell Scientific), stored on a compact flash card, and then processed into half-hourly flux sums using the EddyPro program (LiCor). EddyPro processing was performed using the Express mode. This mode uses the double rotation for the axis rotation for tilt correction, block averaging for turbulent fluctuations, covariance maximum for time lag compensation, 5 standard deviations for vertical velocity and 3.5 standard deviations for CO₂ and H₂O plausibility ranges for the spike count/removal, and the Kljun et al., (2004) footprint analysis.

Meteorological Measurements Micrometeorological variables, including those for interpreting the surface-atmosphere energy balance, were installed at both towers (See Table 1). Canopy heights, and snow depth during the study period (Apr. – Sept.), were measured with a Campbell Scientific SR50A-L sonic depth sensor at the wheat tower. Incident shortwave (SW_{in}), outgoing shortwave (SW_{out}), incident longwave (LW_{in}) and outgoing longwave (LW_{out}) radiation was measured using a NR01 four-component net radiometer (Hukseflux, Delft, The Netherlands). Air temperature (T_a) and humidity (RH) were measured using a HMP45C instrument (Vaisala, Helsinki, Finland). Soil heat flux (G) was measured using a self-calibrating HFP01 heat flux plate (Hukseflux) at 5 cm below the soil surface. Soil moisture was measured at 5 cm and 10 cm using two CS616 sensors (Campbell Scientific) in the wheat field and two CS650 sensors (Campbell Scientific) in the fallow field. Soil temperature was measured at multiple depths using thermocouples in the wheat field and the CS650 sensors in the fallow field. Measurements were made every minute and half-hour averages were stored using CR3000 and CR1000 data loggers (Campbell Scientific).

Gap Filling and Data Processing Missing data occurred due to power outages, equipment malfunction, as well as rodent disturbances to wires. Missing incident shortwave radiation, air and soil temperature, and relative humidity data were gap filled using linear regression from the neighboring tower if data were available. If data from the neighboring tower were also missing, data from the Moccasin SCAN site, located 25 km from the study fields, were used in the gap filling routine.

Gap Filling Latent Heat Flux Data Latent heat flux observations that were missing were gap filled using the Priestley-Taylor model (Priestley and Taylor, 1972).

$$ET_0 = \frac{I}{\lambda} \times \frac{s \times (R_n - G)}{s + \gamma} \times \alpha$$

2.)

Where λ is the latent heat of vaporization, R_n is the net radiation, G is the soil heat flux, s is the slope of the saturation vapor pressure-temperature relationship, γ is the psychrometric constant, and α is the Priestley-Taylor coefficient. The alpha parameter was determined for the SW and fallow sites individually for each day by solving equation 2 for α using measured ET . α , for days on which insufficient data were available for its calculation, was estimated using linear interpolation.

Results and Discussion:

Objective 1:The study period for this project was April 1-Sept. 30, 2014. For this period we found that the soil moisture in the top 10 cm of the soil between the two rotations were not very different (Figure 3). It is unclear if soil moisture in deeper layers differed between wheat and fallow rotations. However, the ET between the two rotations was different. Cumulative ET for the SW crop was 450 mm at the SW field during the measurement period, but reached only 300 mm at the fallow field, *ca.* 1/3 less than the SW field (Figure 4). The 300 mm of ET is seemingly a large number across a fallow field, but Vanderborcht et al. (2010) found in their bare soil evaporation study that measured ET was 77% of potential ET , which makes 300 mm not as surprising. However, the 150 mm difference is nontrivial and represents a half-foot of water that can be used for runoff, deep soil water storage, percolation out of the bottom of the soil column into ground water, or a combination thereof.

Objective 2:An annual measurement of ET was not possible due to power outages and data losses related to rodent disturbances, instrument malfunctions, and severe

weather. However, we are able quantify how *ET* varies as a function of crop growth due to our crop height data provided by the sonic depth sensor. Figure 5 shows the crop height across the study period (April 1-Sept. 30, 2013). Cumulative *ET* for both SW and fallow is *ca.* 35 mm from the date of planting (May 5) to when we see crop height change (May 26). Cumulative *ET* is 275 mm for SW and 124 mm for fallow during the period from the beginning of crop growth on May 26 until maximum height growth on July 25. The last part of the growing season July 25 until crop harvest on Aug 18, we observed a cumulative *ET* of 65 mm in SW and 41 mm in fallow. Based on these findings we can see that wheat and fallow rotations behave similarly before and after crop growth in terms of *ET* with large differences during crop growth at SW.

Objective 3: Due to the fact that we only measured the top 10 cm of the soil we cannot determine the amount of water that moved through the soil column. Instead we will use precipitation as an input and *ET* as an output to determine water that was left available for deep soil moisture, ground water recharge, runoff, or a combination. Total *ET* for the SW and fallow study period was 450 mm and 300 mm which was 90% and 60% respectively of the total precipitation based on the data from the Moccasin SCAN site in 2014 (Figure 7).. In other words, wheat cropping returns almost all incident precipitation to the atmosphere while the fallow sequence leaves over 100 mm available for deep soil water recharge, runoff, or ground water. We would like to note that the Moccasin SCAN site is *ca.* 25 km away from the field sites, and may have seen different precipitation regimes than our field site.

Conclusions:

Based on this one-year study we see minor differences in soil moisture in the top 10 cm between the fallow and SW rotation, while *ET* differed by 150 mm during the April – September study period.

The period of the growing season during which *ET* is most different between the SW and fallow rotations is the period of crop height growth when SW had 151 mm of *ET* more than fallow; most of the cumulative difference during the study period

The precipitation/*ET* ratio between the two rotations was different. SW *ET* returned *ca.* 90% of precipitation to the atmosphere and the fallow returned 60% of the precipitation to the atmosphere.

Overall we see that the differences in *ET* between the two rotations arise during the growth of the crop. The soil moisture measured in the top 10 cm of the soil had negligible differences between SW and fallow rotations. Future studies point to the need of measuring soil moisture at multiple depths to quantify the fate of the water not evapotranspired by fallow, which was on the order of 150 mm.

Table:

Measurement	Sensor	Site Installed
Incoming Shortwave Radiation	NR01 Net Radiometer	SW, F
Outgoing Shortwave Radiation	NR01 Net Radiometer	SW, F
Incoming Longwave Radiation	NR01 Net Radiometer	SW, F
Outgoing Longwave Radiation	NR01 Net Radiometer	SW, F
Canopy Height	SR50 Sonic Distance Sensor	SW
Air Temperature/RH	HMP-50 Temp/RH probe	SW, F
Ground Heat Flux	HFP01 Heat Flux Plate	SW, F
Sensible Heat Flux	CSAT 3 and LI-7200	SW, F
Latent Heat Flux	CSAT 3 and LI-7200	SW, F

Figures:

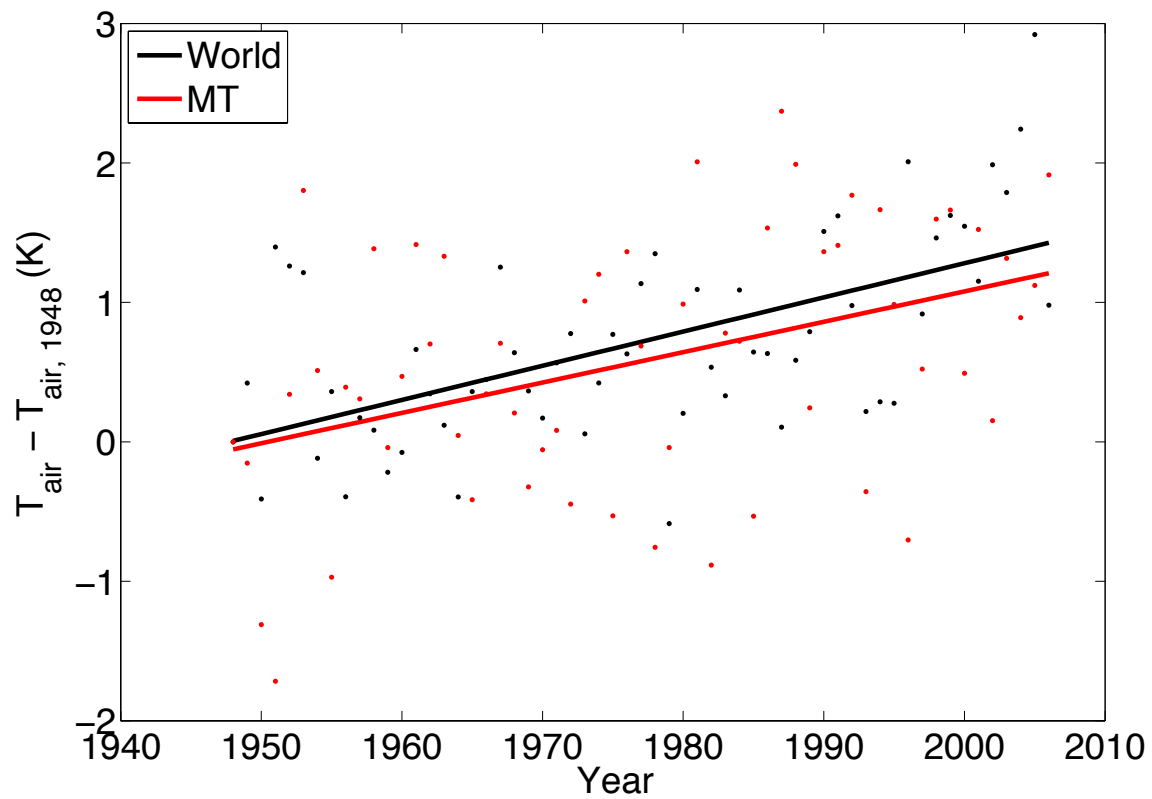


Figure 1: The difference in global and Montana annual air temperature from 1948 following Sheffield et al. (2006).



Figure 2. A map of the winter wheat (2013), spring wheat (2014) and fallow (2014) study sites near Moore, MT in the Judith Basin.

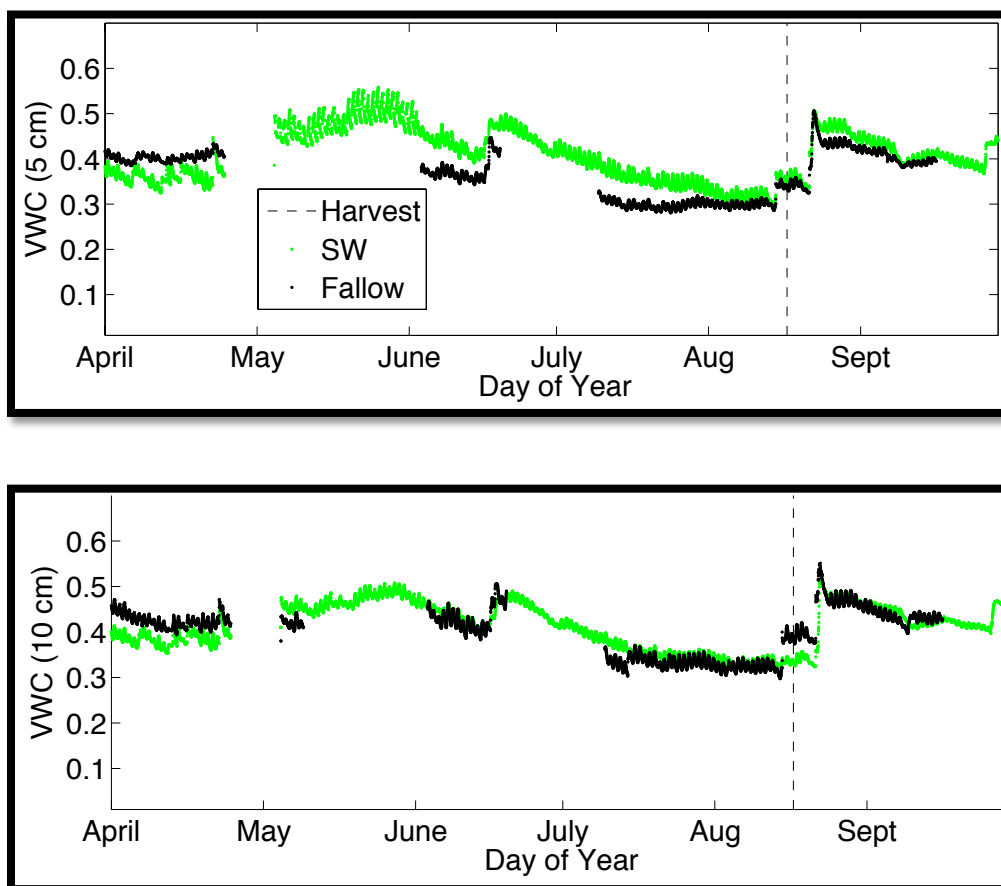


Figure 3: Soil moisture at 5 cm (top) and 10 cm (bottom) below the soil surface for the spring wheat (SW) and fallow study sites near Moore, MT during the April through September 2014 study period. The date of harvest is indicated by the vertical dashed line.

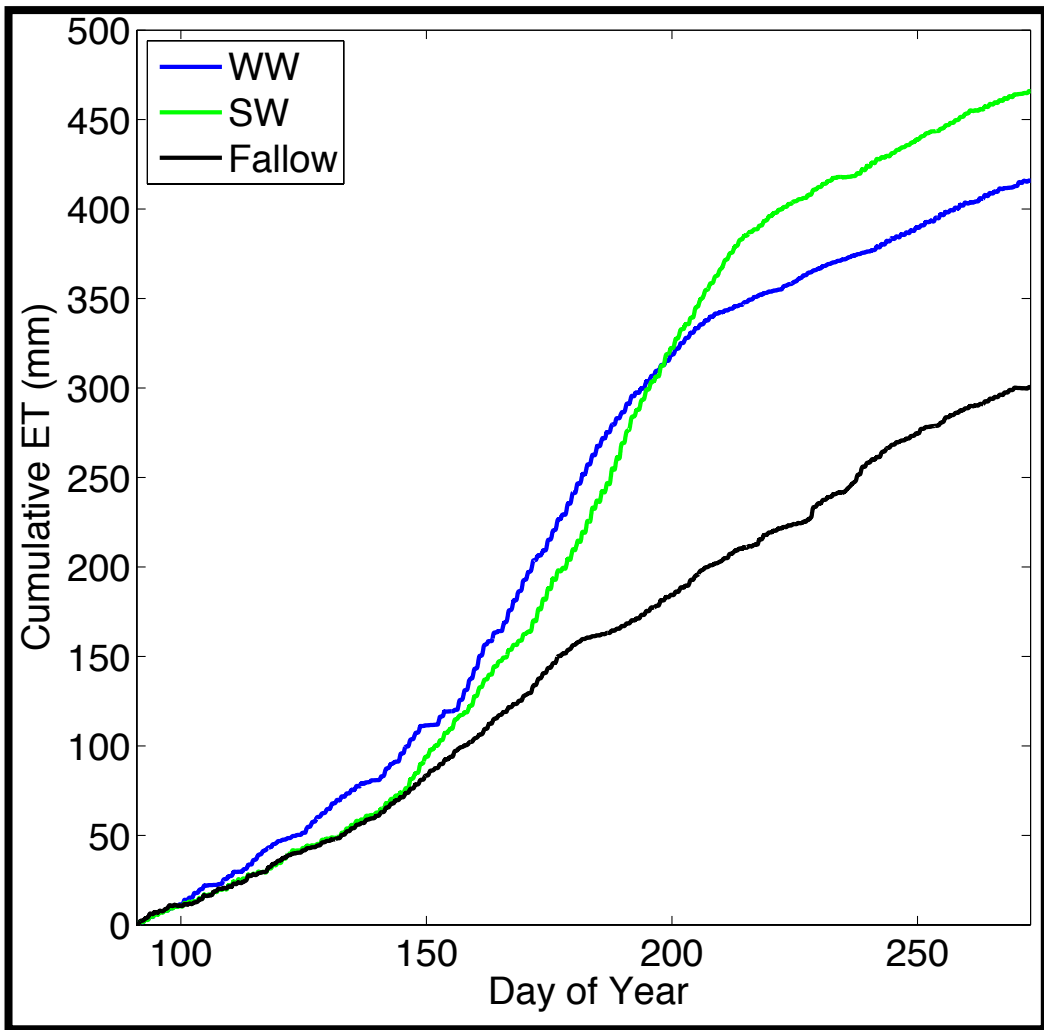


Figure 4. The cumulative sum of evapotranspiration from the winter wheat (WW), spring wheat (SW) and fallow fields during the April-September 2014 study period.

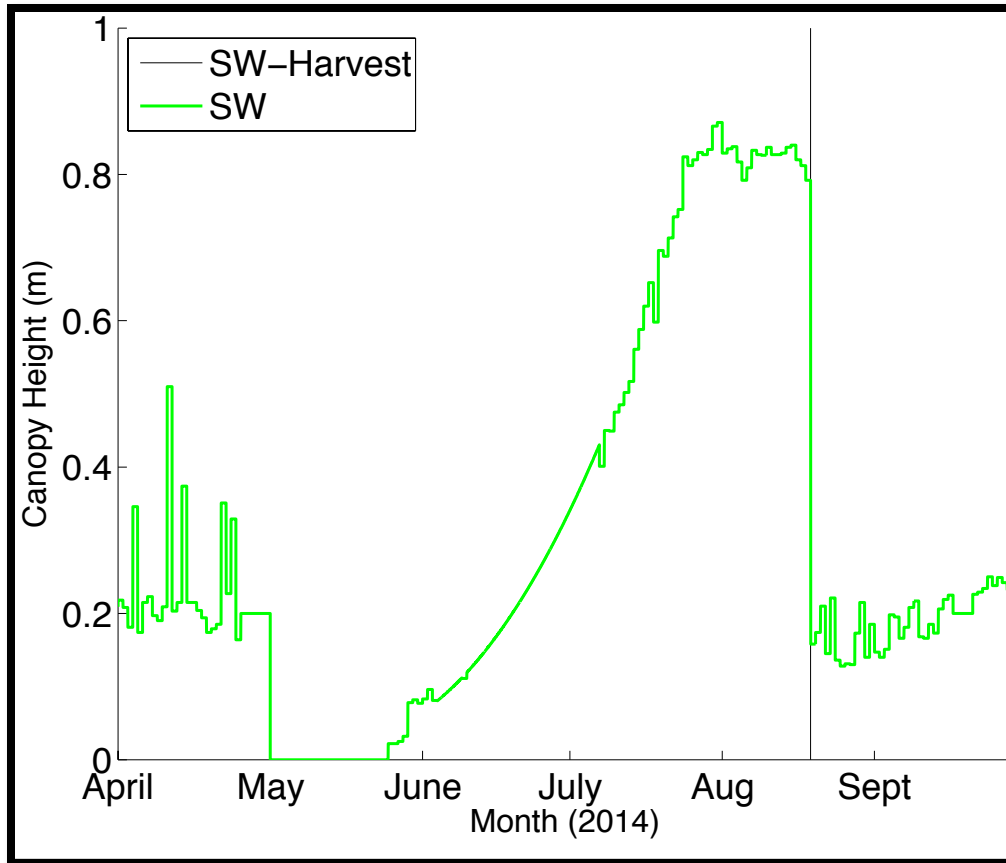


Figure 5: Canopy height in the spring wheat crop during the April – September 2014 study period. The solid gray line denotes the time of harvest.

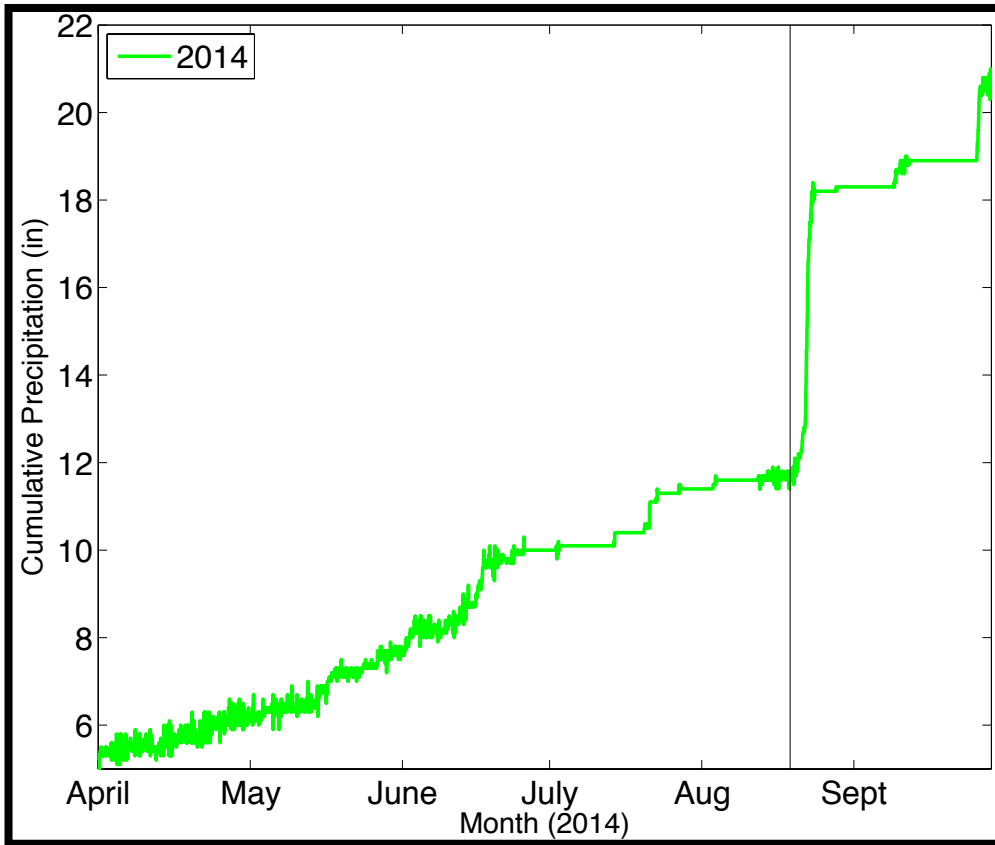


Figure 6: The cumulative sum of precipitation from the Moccasin SCAN site during the April-September 2014 study period.

References:

- Aase, J., Schaefer, G., 1996. Economics of tillage practices and spring wheat and barley crop sequence in the northern Great Plains. *J. Soil Water Conserv.* 51, 167-170.
- Anthoni, P.M., Freibauer, A., Kolle, O., Schulze, E., 2004. Winter wheat carbon exchange in Thuringia, Germany. *Agric. for. Meteorol.* 121, 55-67.
- Asseng, S., Ewert, F., Rosenzweig, C., Jones, J., Hatfield, J., Ruane, A., Boote, K., Thorburn, P., Rötter, R., Cammarano, D., 2013. Uncertainty in simulating wheat yields under climate change. *Nature Climate Change* 3, 827-832.
- Gameda, S., Qian, B., Campbell, C., Desjardins, R., 2007. Climatic trends associated with summerfallow in the Canadian Prairies. *Agric. for. Meteorol.* 142, 170-185.
- Juang, J., Katul, G.G., Porporato, A., Stoy, P.C., Siqueira, M.S., Detto, M., KIM, H., Oren, R., 2007. Eco-hydrological controls on summertime convective rainfall triggers. *Global Change Biol.* 13, 887-896.
- Juang, J., Porporato, A., Stoy, P.C., Siqueira, M.S., Oishi, A.C., Detto, M., Kim, H., Katul, G.G., 2007. Hydrologic and atmospheric controls on initiation of convective precipitation events. *Water Resour. Res.* 43.
- Kljun, N., Calanca, P., Rotach, M., Schmid, H., 2004. A simple parameterisation for flux footprint predictions. *Bound. -Layer Meteorol.* 112, 503-523.
- Luyssaert, S., Jammot, M., Stoy, P.C., Estel, S., Pongratz, J., Ceschia, E., Churkina, G., Don, A., Erb, K., Ferlicoq, M., 2014. Land management and land-cover change have impacts of similar magnitude on surface temperature. *Nature Climate Change* 4, 389-393.
- Priestley, C., Taylor, R., 1972. On the assessment of surface heat flux and evaporation using large-scale parameters. *Mon. Weather Rev.* 100, 81-92.
- Sheffield, J., Goteti, G., Wood, E.F., 2006. Development of a 50-year high-resolution global dataset of meteorological forcings for land surface modeling. *Journal of Climate* 19:3088–3111.
- Vanderborght, J., Graf, A., Steenpass, C., Scharnagl, B., Prolingheuer, N., Herbst, M., Franssen, H.H., Vereecken, H., 2010. Within-field variability of bare soil evaporation derived from eddy covariance measurements special section: patterns. *Vadose Zone Journal* 9, 943-954.

Student Fellowship: Estimating Evapotranspiration at the Regional Scale: An Energy Balance Approach

Basic Information

Title:	Student Fellowship: Estimating Evapotranspiration at the Regional Scale: An Energy Balance Approach
Project Number:	2014MT289B
Start Date:	3/1/2014
End Date:	2/28/2015
Funding Source:	104B
Congressional District:	MT 1
Research Category:	Climate and Hydrologic Processes
Focus Category:	Hydrology, None, None
Descriptors:	None
Principal Investigators:	Aiden Johnson, Aiden Johnson

Publications

There are no publications.

RANDOM UNCERTAINTY IN LAND SURFACE TEMPERATURE CALCULATED USING LANDSAT TM, ETM+, AND TIRS.

Abstract

Quantifying random errors in remotely sensed data products is increasingly important as more scientists from diverse disciplines begin to use these data, often with rudimentary knowledge of how these data products are created and their inherent uncertainties. Most work to date has focused on rigorously assessing and correcting bias errors due to sensor drift atmospheric attenuation, surface properties like land surface emissivity, and other sources, all of which are critical for accurate measurements. Random errors remain after minimizing all known bias terms, but have received less attention to date. To quantify random error in a remotely sensed data product, we apply a Monte Carlo routine to the algorithm used to calculate the land surface temperature (LST) product from Landsat 5 (TM), Landsat 7 (ETM+), and Landsat 8 (TIRS). Specifically, we quantify random uncertainty due to sensor accuracy and the MODTRAN routine used to correct for atmospheric attenuation. A small subset of a Landsat scene within the Judith River watershed in central Montana, USA, was selected for computational efficiency and to avoid the Landsat 7 scan line correction error. The subset represents contains the full range of land cover types present within the watershed including forested upland, crops, and riparian. In order to determine if the Landsat 8 sensor has provided an improved estimate of LST we present two sets of comparisons on days with similar meteorological conditions and prevailing clear skies during the growing season. Day of year 219 (TM) and 211 (TM), 2011, were chosen for the TM/ETM+

comparison, and day of year 184 (ETM+) and 208 (TIRS), 2013 were chosen for the ETM+/TIRS comparison.

For all three Landsat sensors the results indicate the overall uncertainty about the LST product is dominated by random uncertainty and is less a function of the MODTRAN conversion. We find the uncertainty due to the MODTRAN conversion to LST was found to represent between 1.94° K - 4.42° K. The results also indicate no substantial difference in uncertainty depending on sensor or with the advent of Landsat 8, surface properties and conditions are deemed a greater source of uncertainty minimizing the effective difference between sensors. Additionally, we have found that as mean temperature increases overall uncertainty increases. This generally linear relationship of about 1% could be applied to approach quantifying the uncertainty about land surface temperature data at a tertiary level.

Introduction

Remotely-sensed data are subject to bias errors and random errors. Most work to date has focused on rigorously assessing and correcting bias errors due to sensor drift (Barsi, Barker, & Schott, 2003), atmospheric attenuation (Barsi et al. 2003), surface properties like land surface emissivity, and other sources, all of which are critical for accurate measurements. Random errors remain after minimizing all known bias terms, but have received less attention to date.

Quantifying random errors in remotely sensed data products is increasingly important as more scientists from diverse disciplines begin to use these data, often with rudimentary knowledge of how these data products are created and their inherent uncertainties. Quantifying uncertainty in remotely sensed data products is also important for scientific objectives. Uncertainty estimates are required, for example, to implement data assimilation routines (Hill, Quaife, & Williams, 2011), bridge scales between ground-based and space-based observations (Jarvis, 1995; Stoy, Williams, & Disney, 2009), and detect significant temporal and spatial changes in land surface attributes (Prieto-Blanco, et al. 2009; Kerr & Ostrovsky 2003; Cohen & Goward 2004; Tan, Masek, & Wolfe, 2013). Quantifying random errors, in addition to bias errors, is necessary for a full accounting of uncertainty, and communicating these uncertainties to the ever-growing community of remote sensing data product users is important for appropriate and informed usage of these data.

To quantify random error in a remotely sensed data product, we apply a Monte Carlo routine to the algorithm used to calculate the land surface temperature (LST) product from Landsat 5 (TM), Landsat 7 (ETM+), and Landsat 8 (TIRS). Specifically, we quantify random uncertainty due to sensor accuracy and the MODTRAN routine used to correct for atmospheric attenuation to address the following questions:

- (1) How has the random uncertainty in the LST product changed with advent of new satellites in the Landsat constellation?
- (2) Which is a greater source of uncertainty, the satellite observations themselves or the atmospheric corrections used to calculate the LST data product?

(3) Is it possible to create a simple estimate of random uncertainty based on the magnitude of LST?

We focus our analysis on a gradient between agriculturally-dominated landscapes, rangeland, and forest to encompass a wide range of surface types while avoiding the known scan line correction error in Landsat 7 (Coll, 2010).

Materials and Methods

Study Site

The study site is in the Judith River watershed in central Montana. The Judith River headwaters are dominated by montane coniferous forests, and dryland cereal and forage production dominate at lower elevations. A small subset within the Judith River watershed was selected for computational efficiency and to avoid the Landsat 7 scan line correction error. The subset represents a transect from forested upland to cropland and riparian areas and was chosen to include the full range of land cover types present within the watershed. The spatial extent of the study area is 330 km² and includes an eddy flux tower located at 46.994701 N, 109.613660 W (Figure 3.1).

Landsat Data

Landsat data were downloaded from the USGS GLOVIS website. Landsat TM and ETM+ data were downloaded for the 2011 growing season for comparison, and Landsat ETM+ and TIRS data were downloaded for the 2013 growing season. As Landsat TM was unavailable after Autumn 2011, and therefore cannot be directly compared to Landsat 8 for which data became available on February, 2013, we

present two sets of comparisons on days with similar meteorological conditions and prevailing clear skies during the growing season. Day of year 219 (TM) and 211 (ETM+), 2011, were chosen for the TM/ETM+ comparison, and day of year 184 (ETM+) and 208 (TIRS), 2013 were chosen for the ETM+/TIRS comparison. All three sensors provide multispectral data with 30 m spatial resolutions and are described in detail elsewhere (Irish 2000).

Data from each date was first converted to digital numbers from at sensor brightness then using MODTRAN (Eq.1) and Eq. 2. converted to land surface temperature by applying adjustments for atmospheric attenuation outlined by (Barsi et al. 2003). Uncertainty in the MODTRAN atmospheric adjustment is within 2-3 degrees K (Quattrochi and Luvall 2004). Moderate resolution atmospheric Transmission (MODTRAN) is a computer program originally written in Fortran, used to model atmospheric attenuation and propagation of electromagnetic energy through the atmosphere, it was developed by the U.S. Air force and is maintained by several US agencies. The equation for calculation is given here:

$$L_{TOA} = \tau \varepsilon L_T + L_u + (1 - \varepsilon)L_d \quad (1)$$

where τ is the atmospheric transmission, ε is the emissivity of the surface, L_T is the radiance of a blackbody target of kinetic temperature T , L_u is the upwelling or atmospheric path radiance, L_d is the downwelling or sky radiance, and L_{TOA} is the space-reaching or TOA radiance measured by the instrument. Radiances are in units of $W/m^2ster \cdot \mu m$ and the transmission and emissivity are unitless. Landsat radiances were then converted to land surface temperature in Kelvin following Chander, Markham, & Helder (2009):

$$LST = K_2 \ln(K_1 L\lambda) \quad (2)$$

where K_1 and K_2 are calibration constants that differ among sensors (see Table 3.2) and $L\lambda$ is spectral radiance leaving the Earth's surface. K_1 and K_2 are derived from Planck's Law and contribute little random uncertainty to the final LST product. The LST product can be seen in Figure 3.2 as it is generated following the MODTRAN adjustment and Planck's law conversion to temperature. This is the land surface temperature data typically used in remote sensing studies that require the spatial scale of Landsat (30 m) rather than MODIS or some other larger spatial scaled temperature data.

Monte Carlo Uncertainty Analysis

There are two primary sources of random uncertainty in Landsat-derived LST: uncertainty in the raw digital remote sensing values and uncertainty in the MODTRAN estimate of atmospheric attenuation across the thermal bands. To quantify the uncertainty associated with sensor measurements and atmospheric attenuation in Eq. (1), a Monte Carlo method of random parameter generation was applied. The Monte Carlo approach applied here uses a defined distribution, here a Gaussian distribution with variance of 2° Kelvin as found by (Quattrochi and Luvall 2004), and random draws to select multiple realizations of likely parameter sets and the subsequent MODTRAN parameters of L_d , L_u , and τ . One thousand iterations of the MODTRAN values were created for each pixel of each Landsat scene subset the resulting distributions are shown in Figure 3.3. We assume that the parameter values K_1 and K_2 contribute trivial amounts of uncertainty – apart from rounding error - as they are calculated directly from Planck's Law.

The next step was to generate LST products for each sensor subset using the distributions of values and finding the means and variances of the stacks of images for each sensor. In, Figure 3. 3 we have the mean LST's in upper four panels and variances in lower four panels. Here we can compare the range of values for each sensor and their associated variance. The temperatures range from 310° K - 289° K, well within what would be expected for this region and season. The variances are also quite similar across sensor, excluding the ETM 211, ranging from 2° K to 4.5° K, but with most of pixels falling in the less than 4 degrees range. Similarly if we subtract the mean LST images generated from the MC routine from the LST images generated by the specific MODTRAN suggested adjustments we can see in Figure 3.4 there is little difference in the results across sensors, illustrating the effect of added uncertainty from MODTRAN is minimal and the real difference in variance has more to do with the specific image itself.

Results

Uncertainty due to the MODTRAN conversion to LST was found to represent between 1.94° K - 4.42° K, see Table 3.3. For both Landsat TM and ETM+ this result indicates the overall uncertainty about the LST product is dominated by random uncertainty and is less a function of the MODTRAN conversion.

Uncertainty within Subsets of Landsat Scenes

Maps of calculated LST for both study dates are presented in Figure 3.3 & 3.4. The mean temperatures are similar across both comparisons three sensors, as they are seasonally similar. The maps provide some contextual perspective; we can see

the warmer temperatures are found in the croplands and rangeland areas, where as the cooler areas are the riparian and slightly elevated forested areas in blues. There is also a single pivot irrigated field which is also bright blue and subsequently *ca.* 10° K cooler than the surrounding areas for all images.

The results indicate there is no significant decrease in the uncertainty in transition from TIRS to ETM+. These analyses found a decrease in uncertainty in Landsat ETM+ as compared to its predecessor Landsat TM. Figure 3.3 displays the mean and variance for each Landsat sensors for the subset region. The proportion of uncertainty associated with MODTRAN was fairly consistent increasing slightly when total variance increased in the scene and as temperatures increased as well. Reviewing Figure 3.4 we can see the remaining variability after taking the difference between the date specific MODTRAN calculated LST and the Monte Carlo simulated mean LST.

Discussion

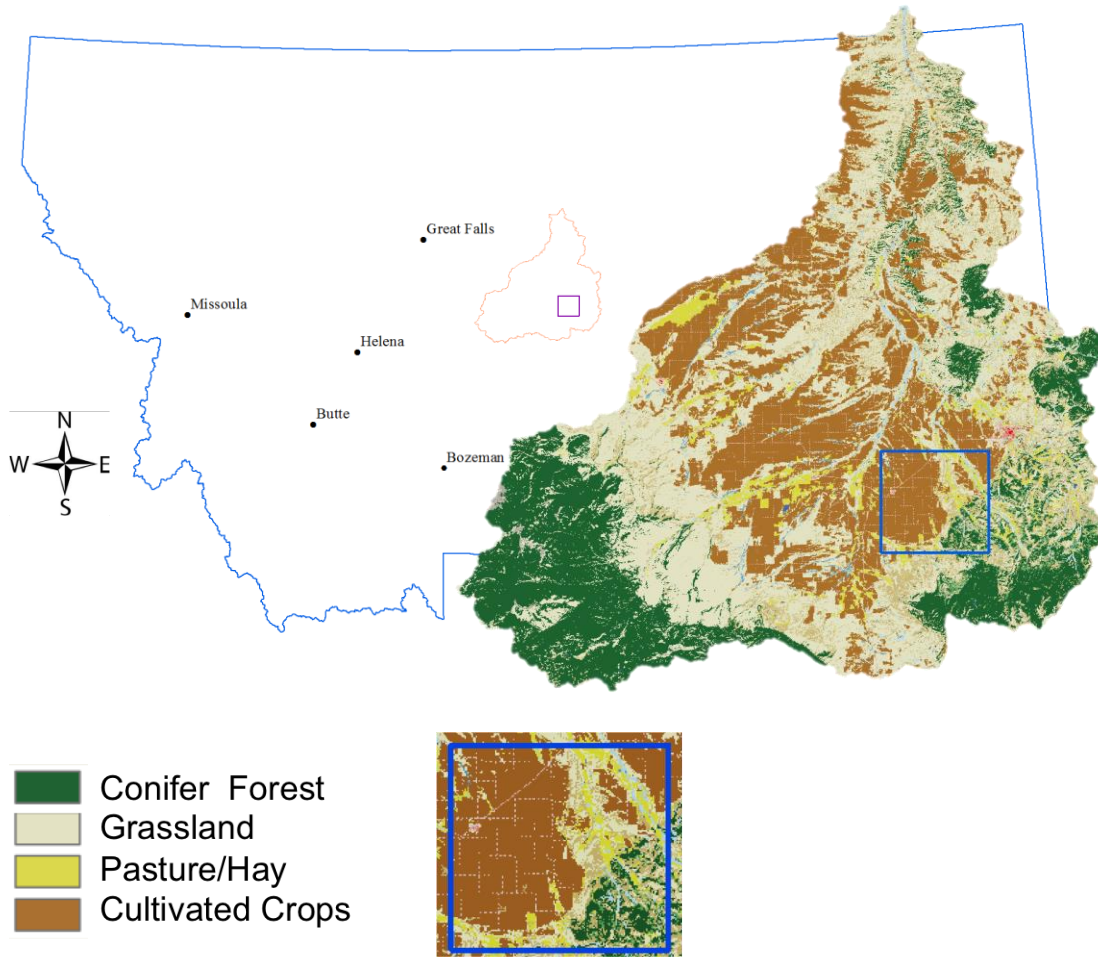
The improvements in sensor design in Landsat TIRS for thermal band are a significant finding that should be considered for any future land surface temperature analyses. It is clear that Landsat TIRS has improved in terms of uncertainty not associated with the MODTRAN translation; however, it cannot be clearly distinguished as an improvement in the sensor versus a general landscape decrease in variance for the time period reviewed. Future analysis should involve multiple landscapes and climatic regions for transferability analysis of findings.

The non-linear relationship of the MODTRAN correction has resulted in an increase width in the distribution of values for land surface temperature. This method of radiative transfer in order to incorporate atmospheric attenuation adjustment is expected to cause an increase in the land surface temperature uncertainty however this is necessary adjustment to gain a value for temperature at the surface of the Earth.

The data themselves are found to be the greatest source of uncertainty in these analyses. Relying on atmospheric adjustments and Planck's law translations does not substantially impact the resulting land surface data negatively.

Additionally, we have found that as mean temperature increases overall uncertainty increases. This generally linear relationship of about 1% could be applied to approach quantifying the uncertainty about land surface temperature data at a tertiary level.

The level of uncertainty found in these land surface temperature analysis can be extended to other Landsat derived data products. The linear relationships linking spectral responses to biophysical properties always have an associated uncertainty. Understanding and reporting the variance associated with derived products is necessary for interpretation of actual change versus randomness. The level of estimated uncertainty helps elucidate the reasonable level of inference for a Landsat derived data products.



1500 m

Figure 3.1: The Judith Watershed (inset) in the U.S. State of Montana. The lower center subplot represents a land cover classification of the study domain (highlighted in blue).

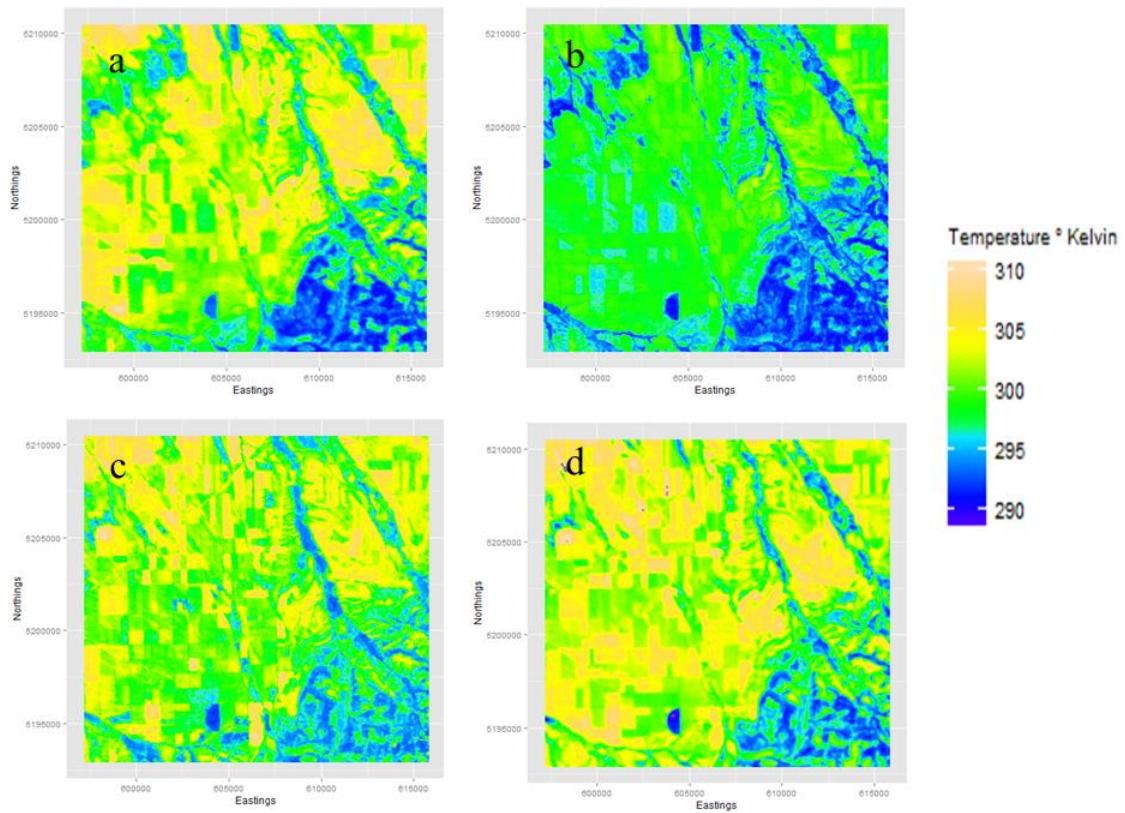


Figure 3.2. Land surface temperature in Kelvins, (a) Landsat TM mean LST August 7, 2011. (b) Landsat ETM+ LST July 30, 2011(c) Landsat ETM+ LST July 3, 2013. (d) LST from Landsat TIRS on July 27, 2013.

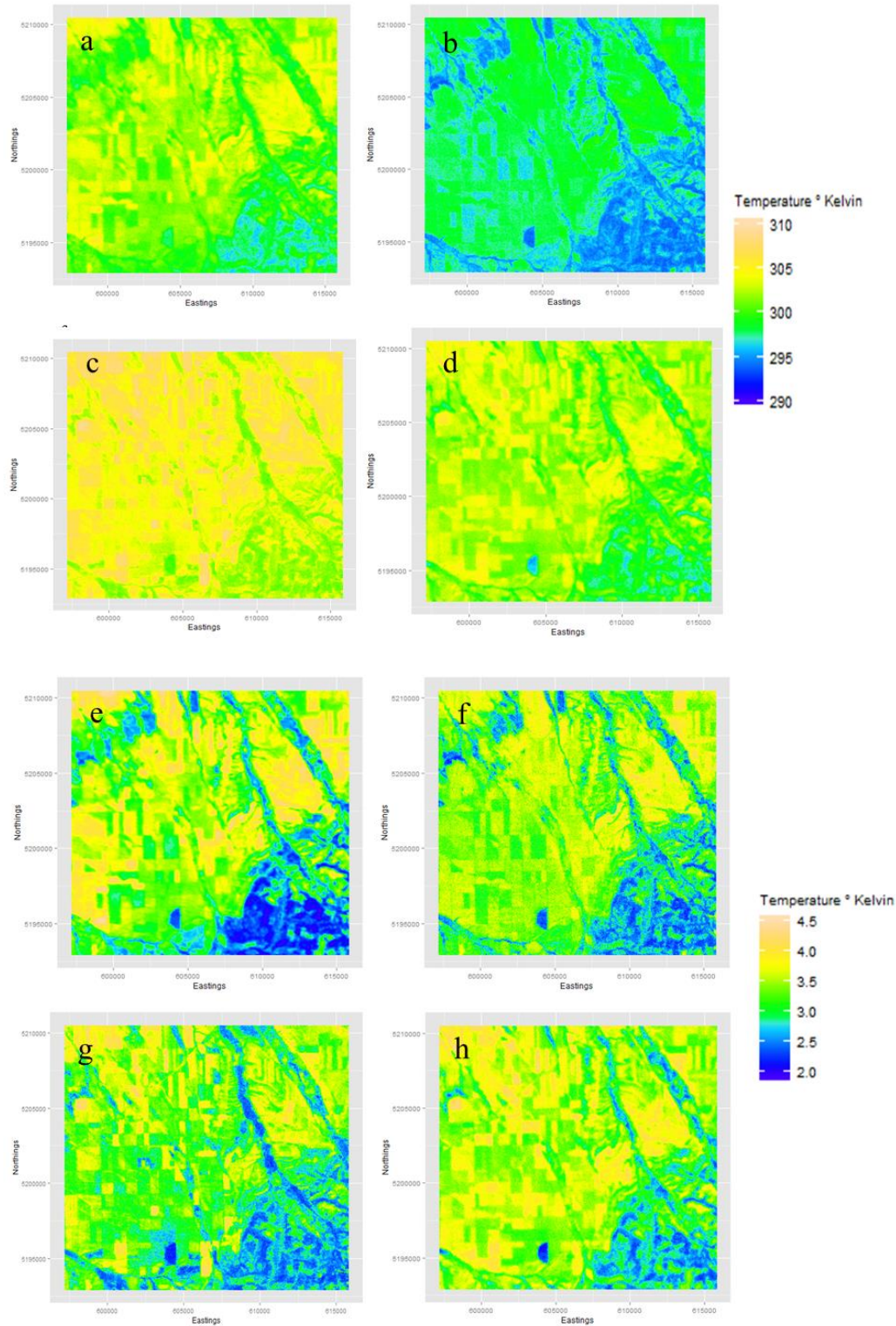


Figure 3.3. Mean and variance of LST layers created through Monte Carlo simulation of the parameters of MODTRAN. Mean images are shown on the left and variances on the right. (a) and (e) Landsat TM mean LST and variance of LST layers

respectively, for August 7, 2011. (b) and (f) Landsat ETM+ July 30, 2011. (c) and (g) Landsat ETM+ July 3, 2013. (d) and (h) Landsat TIRS data from July 27, 2013.

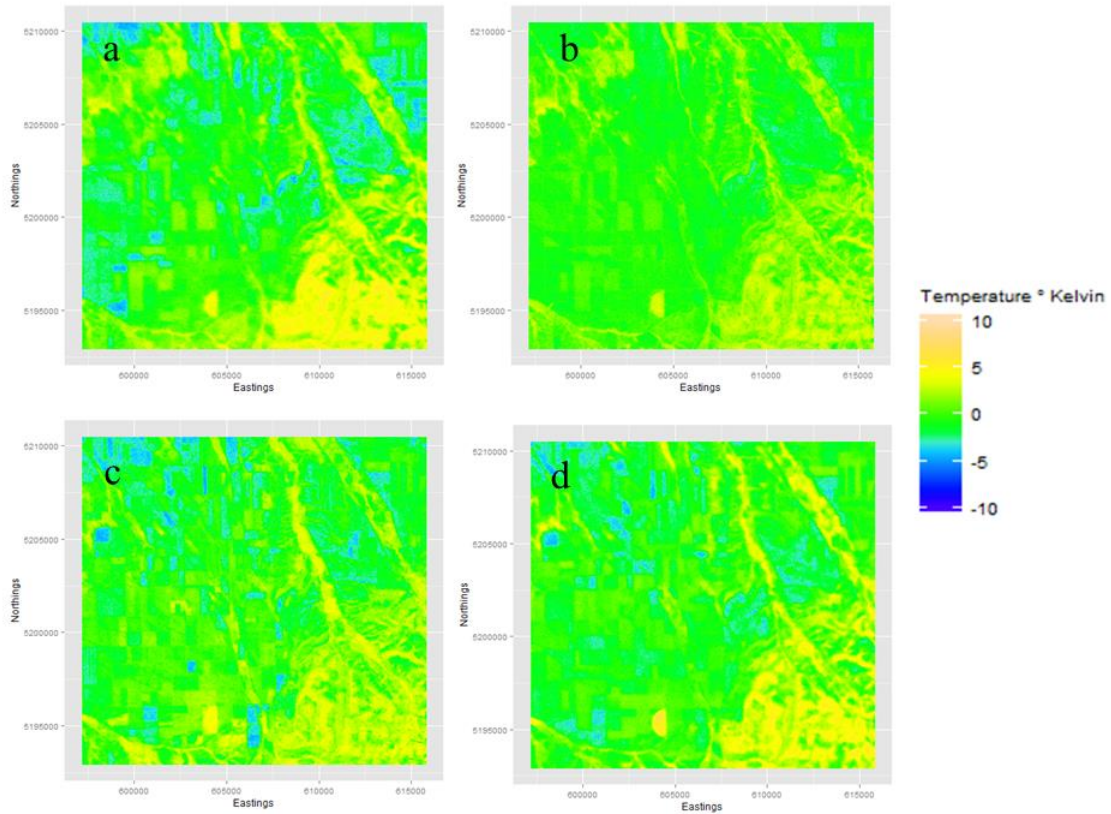


Figure 3.4. (a) Image differences in LST created from date specific adjustments and mean LST from Monte Carlo simulation of parameters for Landsat TM DOY 219 2011. (b) Image differences in LST created from date specific adjustments and mean LST from Monte Carlo simulation of parameters for Landsat ETM+ 211, 2011. (c) Image differences in LST created from date specific adjustments and mean LST from Monte Carlo simulation of parameters for Landsat ETM+ 184 2013. (d) Image differences in LST created from date specific adjustments and mean LST from Monte Carlo simulation of parameters for Landsat TIRS on DOY 208 2013.

Table 3.1. Data Attributes

Landsat Thermal data				
Satellite Name	Band Number	Wavelength (micrometers)	Sampled Resolution	Pixel Resolution
Landsat-5 TM	6	10.40-12.50	120m	30m
Landsat-7 ETM+	6	10.31-12.36	60m	30m
Landsat-8 TIRS	10	10.6-11.19	100m	30m

Table 3.2. Data Table

Sensor	DOY	Date	Year	K1	K2
TM	219	7-Aug	2011	607.76	1260.56
ETM+	211	30-Jul	2011	666.09	1282.71
ETM+	184	3-Jul	2013	666.09	1282.71
L8	208	27-Jul	2013	774.89	1321.08

Table 3.3. Variances in Degrees Kelvin

Sensor	DOY	Total Variance	Variance of LST	Percent Variance from MODTRAN	Random Variance
TM	219	61.1	4.42	7.23	56.68
ETM+	211	7.19	1.94	9.61	5.25
ETM+	184	33.7	3.24	26.98	30.46
TIRS	208	40.1	3.56	8.88	36.54

Acknowledgements

The Montana Institute on Ecosystems provided financial assistance. PCS acknowledges funding from the National Science Foundation ('Scaling ecosystem function: Novel Approaches from MaxEnt and Multiresolution', Division of Biological Infrastructure #1021095), the State of Montana, the Montana Water Center, and the U.S. Geological Survey.

References

1. Barsi JA, Barker JL, Schott JR (2003) An atmospheric correction parameter calculator for a single thermal band earth-sensing instrument. *Geosci. Remote Sens. Symp. 2003. IGARSS'03. Proceedings. 2003 IEEE Int. IEEE*, pp 3014–3016
2. Barsi JA, Hook SJ, Palluconi FD, et al. (2006) Landsat TM and ETM+ thermal band calibration. *SPIE Opt. Photonics. International Society for Optics and Photonics*, p 62960F–62960F
3. Chander G, Markham BL, Helder DL (2009) Summary of current radiometric calibration coefficients for Landsat MSS, TM, ETM+, and EO-1 ALI sensors. *Remote Sens Environ* 113:893–903. doi: 10.1016/j.rse.2009.01.007
4. Cohen WB, Goward SN (2004) Landsat's role in ecological applications of remote sensing. *Bioscience* 54:535–545.
5. Coll, César, et al. "Validation of Landsat-7/ETM+ thermal-band calibration and atmospheric correction with ground-based measurements." *Geoscience and Remote Sensing, IEEE Transactions on* 48.1 (2010): 547-555.
6. Hill TC, Quaife T, Williams M (2011) A data assimilation method for using low-resolution Earth observation data in heterogeneous ecosystems. *J Geophys Res* 116:D08117. doi: 10.1029/2010JD015268
7. Irish RR (2000) Landsat 7 science data users handbook. *Natl Aeronaut Sp Adm Rep* 415–430.
8. Jarvis, P. G. "Scaling processes and problems." *Plant, Cell & Environment* 18.10 (1995): 1079-1089.
9. Kerr JT, Ostrovsky M (2003) From space to species: ecological applications for remote sensing. *Trends Ecol Evol* 18:299–305.
10. Prieto-Blanco, Ana, et al. "Satellite-driven modelling of net primary productivity (NPP): theoretical analysis." *Remote Sensing of Environment* 113.1 (2009): 137-147.
11. Quattrochi DA, Luvall JC (2004) *Thermal Remote Sensing in Land Surface Processing*. Taylor & Francis
12. Stoy PC, Williams M, Disney M, et al. (2009) Upscaling as ecological information transfer: a simple framework with application to Arctic ecosystem carbon exchange. *Landsc Ecol* 24:971–986. doi: 10.1007/s10980-009-9367-3

13. Tan B, Masek JG, Wolfe R, et al. (2013) Improved forest change detection with terrain illumination corrected Landsat images. *Remote Sens Environ* 136:469–483.

Student Fellowship: Precipitation and topographic controls over montane forest transpiration

Basic Information

Title:	Student Fellowship: Precipitation and topographic controls over montane forest transpiration
Project Number:	2014MT290B
Start Date:	3/1/2014
End Date:	2/28/2015
Funding Source:	104B
Congressional District:	MT 1
Research Category:	Climate and Hydrologic Processes
Focus Category:	Hydrology, None, None
Descriptors:	None
Principal Investigators:	Justin Martin

Publications

There are no publications.

Differential Use of Water from Rain and Snow by Rocky Mountain Conifers

Justin Martin

April 21, 2015

Contents

Overview	3
Methods	3
Results	4
Discussion	5
References	12

List of Tables

1	Model output [ref. pg. 5]	5
---	-------------------------------------	---

List of Figures

1	Study Design [ref. pg. 3]	6
2	Local Meteoric Water Line [ref. pg. 3]	7
3	Species Differences in Xylem [ref. pg. 4]	8
4	Soil Isotope Profiles [ref. pg. 4]	9
5	Species and Soil Isotopes [ref. pg. 4]	10
6	Topographic position vs. Percent Snow [ref. pg. 5]	10
7	Fitted values vs twi [ref. pg. 5]	11

Overview

Dear Water Center,

Thank you again for supporting my research into forest water use in Montana. The past year has proven quite productive in terms of gathering and processing samples and synthesizing data. With the help of a fantastic team of undergraduate research assistants, I have completed a second year of sample collection bringing our total number of tree, soil, and precipitation isotope samples to approximately 1200. We have been continuously processing these samples for the past year and now have a relatively complete picture of tree water use at the Lubrecht Experimental Forest for 2013. Within several months, we hope to have finished processing all of the samples collected during 2014 as well and we will then be able to contrast tree water use over two distinctly different precipitation years. I am also continuing sample collection for 2015 which will help to characterize tree water use following a very low snow year at Lubrecht.

My original proposal posed three questions as follows:

Q1- Does the proportion of transpired water attributable to rain/snow differ by tree species depending on the species ability to use water from snowmelt vs. summer rains?

Q2- Does the proportion of transpired water attributable to rain/snow differ by topographic position depending on the differential behavior of these source waters after infiltration?

Q3- Can field based and remotely sensed estimates of biomass, stand composition, and topography be used to scale tree level measurements of transpiration and the spatial and temporal distribution of its source waters to the watershed level?

To date, I feel we have a good handle on questions 1 and 2. As the determination of transpiration alone is enough to keep a master's student busy for several years, my colleague Nate Looker is spearheading the transpiration work for our project. This has left me with the task of characterizing the source of waters present in the sap stream of trees over the growing season using the isotopic approach described in my original proposal and the results of this work are presented below. We will soon be combining Nate's findings with mine to determine how different precipitation inputs contributed to the overall forest transpiration flux and how these inputs are mediated by physiological differences between species and topographic effects. I will continue to explore the feasibility of question 3 as an additional chapter in my dissertation and work will begin in earnest on this aspect of the project during the spring of 2016.

Methods

To address questions 1 and 2, water samples from rain, snow, streams (Figure 2), soils, and seventy-two trees were collected, with 34 trees sampled at a low elevation of ~ 1500 m and 38 trees sampled at a higher elevation of ~ 2100 m (Figure 1). Trees were not randomly selected from the landscape but were instead chosen to represent the range of possible TWI and insolation values present at each elevation. Random selection of trees was not possible because of the desire to instrument them with wired sensors in the future, limiting the possible distance between them. Only two elevations were sampled due to vehicle access constraints within the study watershed and as such elevation is treated as a categorical explanatory variable for the fraction of xylem water originally from rain (f). The rooting depth of trees may have been confounding factor influencing a tree's access to different water

sources that was impossible to directly measure. To attempt to control for this, I included each tree's diameter at breast height (DBH) in potential models for the analyses assuming that rooting depth was generally proportional to tree size. Species differences are addressed here graphically while topographic differences are assessed via a multiple regression approach accounting for tree size, site elevation, and solar insolation.

Water samples were analyzed for stable isotopes of oxygen and hydrogen ($\delta^{18}\text{O}$ and δD) and were used to estimate the fraction of xylem water from rain vs snow (f), using a two end member mixing model as follows:

$$\delta\text{D}/18\text{O} = (R_{\text{sample}} / R_{\text{standard}} - 1) \times 1000 \quad (1)$$

where R_{sample} and R_{standard} are the molar ratios of $\delta^{18}\text{O}/16\text{O}$ and $\delta\text{D}/\text{H}$ of the sample and standard water (V-SMOW) respectively,

$$f = (\delta\text{D}_{\text{xylem}} - \delta\text{D}_{\text{snow}}) / (\delta\text{D}_{\text{rain}} - \delta\text{D}_{\text{snow}}) \quad (2)$$

where $\delta\text{D}_{\text{xylem}}$, $\delta\text{D}_{\text{rain}}$, and $\delta\text{D}_{\text{snow}}$ are the isotopic composition of the xylem water, rainwater, and snow melt, respectively, and f is the fraction of rainwater in the xylem.

A first order control on water availability in complex landscapes is the area of land upslope of any given location that contributes to sub-surface flow at that point. This contribution was estimated by a metric known as the topographic wetness index (TWI) in which $\text{TWI} = \ln(a/\tan B)$ where a = the upslope contributing area in m^2 and B = slope in degrees. In addition, the response of montane forests to changes in precipitation regimes will likely vary at different elevations and across gradients of slope aspect which primarily influences the amount of solar radiation intercepted by a given location (insolation) and which is estimated here from a LiDAR derived digital elevation model [1].

Results

Question 1: Species differences in source waters observed in xylem appear to be relatively clear at certain times of year (Figure 3). In particular, Western Larch and Ponderosa pine appear to access water derived primarily from snowmelt (more negative ^{18}O values) although likely for very different physiological reasons. One possible reason is that species are accessing moisture from different soil moisture pools. Figure 4 shows oxygen isotope ratios from the six sampled soil depths at each site over time. Increasing evidence of evaporative enrichment of, and inputs of more isotopically positive precipitation to surface soils over time allow us to track the depth of soil moisture pools accessed by trees. Species appear to access water from different depths depending on the availability of moisture at different depths. This is especially evident in the case of Ponderosa pine which occupies the driest locations and accesses water from increasingly deep soils as moisture becomes more scarce. We observe an increasing disparity between xylem water and surface soil moisture isotopic values as conditions dry (Figure 5). During the same period, Western Larch consistently access more negative waters at depth regardless of conditions in near surface soils. Other species seem to track relatively closely with isotope values from surface soils implying that these trees continue to access water from near surface soils. As I have observed large differences in sapwood depth between species at the same site, I would like to include this variable in future analyses as such differences imply potentially different access to soil moisture pools. A more rigorous statistical comparison of species will follow characterization of sapwood depth this summer.

Question 2: In general, trees at lower elevation, and trees growing in hollow positions relied more heavily on snowmelt than trees growing at high elevation and trees growing on slopes (Figure 6). To address the influence of topography on source water in xylem in terms of twi, the linear model $\mu = \{f \mid \text{elevation, sqrt(radiation), dbh, log(twi)}\} = \beta_0 + \beta_1 * \text{elevation} + \beta_2 * \text{sqrt(radiation)} + \beta_3 * \text{dbh} + \beta_4 * \text{log(twi)} + \beta_5 * \text{dbh:log(twi)}$ was fit to the data from 72 trees. There is weak evidence to suggest that the relationship between twi and f depends on elevation, (p-value = 0.769 from an ESS F-test with an F-stat = 0.087 on 1 and 65 df). There is moderate evidence to suggest that the relationship between twi and f depends on tree size (dbh), (p-value = 0.037 from an ESS F-test with an F-stat = 4.529 on 1 and 66 df). It is estimated that a 1% increase in twi is associated with an average 0.003 + 0.005* dbh unit decrease in f after accounting for radiation and elevation, with an associated 95% confidence interval of (0.005 + 3e-04* dbh unit decrease to a 0.001 + 0.011* dbh unit decrease) (Table 1, Figure 7).

	Estimate	Std. Error	t value	Pr(> t)
(Intercept)	1.1646	0.2038	5.72	0.0000
elevationlow	-0.1141	0.0259	-4.41	0.0000
sqrt.radiation	0.0003	0.0003	1.04	0.3000
dbh	-0.0132	0.0056	-2.36	0.0211
log.twi	-0.2716	0.0947	-2.87	0.0055
dbh:log.twi	0.0055	0.0026	2.13	0.0371

Table 1: Model output [ref. pg. 5]

Discussion

To date, I am unsure of what contributes to differences in tree water use between species, however location appears to play some role. Ponderosa pine and Western Larch are the most unique species in terms of (f) and also occupy the most limited range on conditions with Ponderosa pine occupying only the driest sites and Western Larch, only the wettest. Further analysis of where in the soil profile each species is accessing water and the local moisture conditions at that particular time is needed to develop hypotheses about potential drivers of interspecies variation. In addition, by combining isotope data with transpiration measurements from each species I hope to better understand how differences in water demand might effect sourcing of water from soils in different species occupying similar locations.

It is somewhat counter-intuitive but quite interesting that trees at low elevations rely more heavily on snowmelt than trees at high elevation. We know from meteorological data collected on site that the low elevations have lower soil moisture and higher atmospheric demand for moisture in terms of vapor pressure deficit. We also see that trees in the very driest locations rely more on snow melt (Ponderosa pine). In light of this, it is sensible to think that trees living in dry locations adapt via rooting depth to access more consistent soil moisture at depth. This pool of soil moisture is also primarily recharged by spring snowmelt as summer rains rarely penetrate far enough to contribute moisture to deeper soils. Differences in rooting depth may also explain why larger trees rely more on snow than smaller trees.

Topography seems to independently influence tree water use as well. We see that trees growing on slopes are more dependent on rain than trees in hollows. Slope soils become very dry even at depth

during the summer and trees on slopes may need to take better advantage of short summer rains than trees in hollows with more consistent water supplies. These hollow trees likely have access to flow paths that continue to contribute snowmelt to streamflow downslope throughout the growing season via lateral re-distribution. Lastly, small trees likely lack root systems needed to access deep water regardless of topographic position and may rely more heavily on rains and near surface soil moisture to meet their demand for water. Again, by combining isotope and transpiration measurements in the future, I hope to develop a clearer picture of what role a tree's transpirational demand plays in its sourcing of water from soils as is mediated by topography.

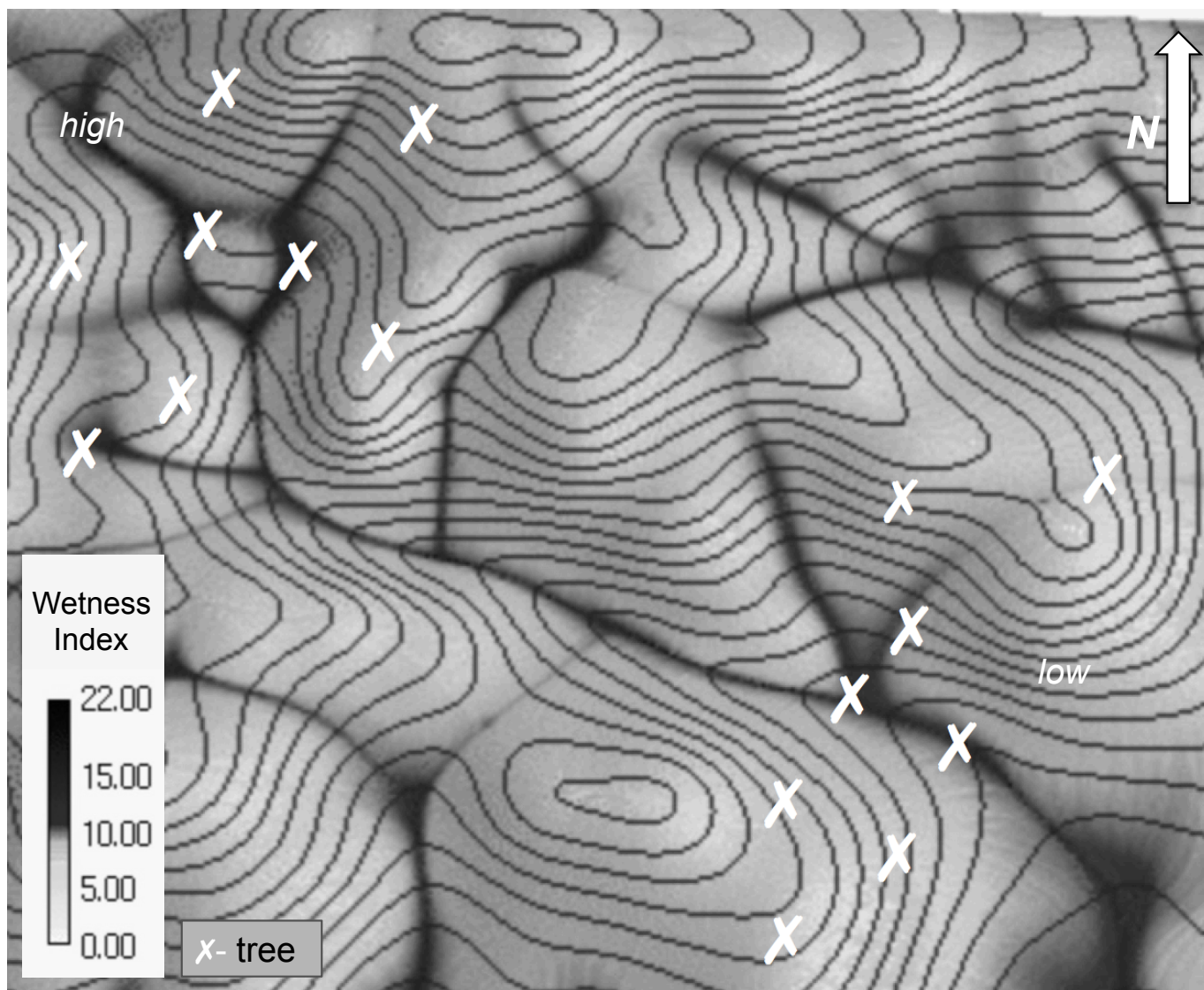


Figure 1: Study Design [ref. pg. 3]

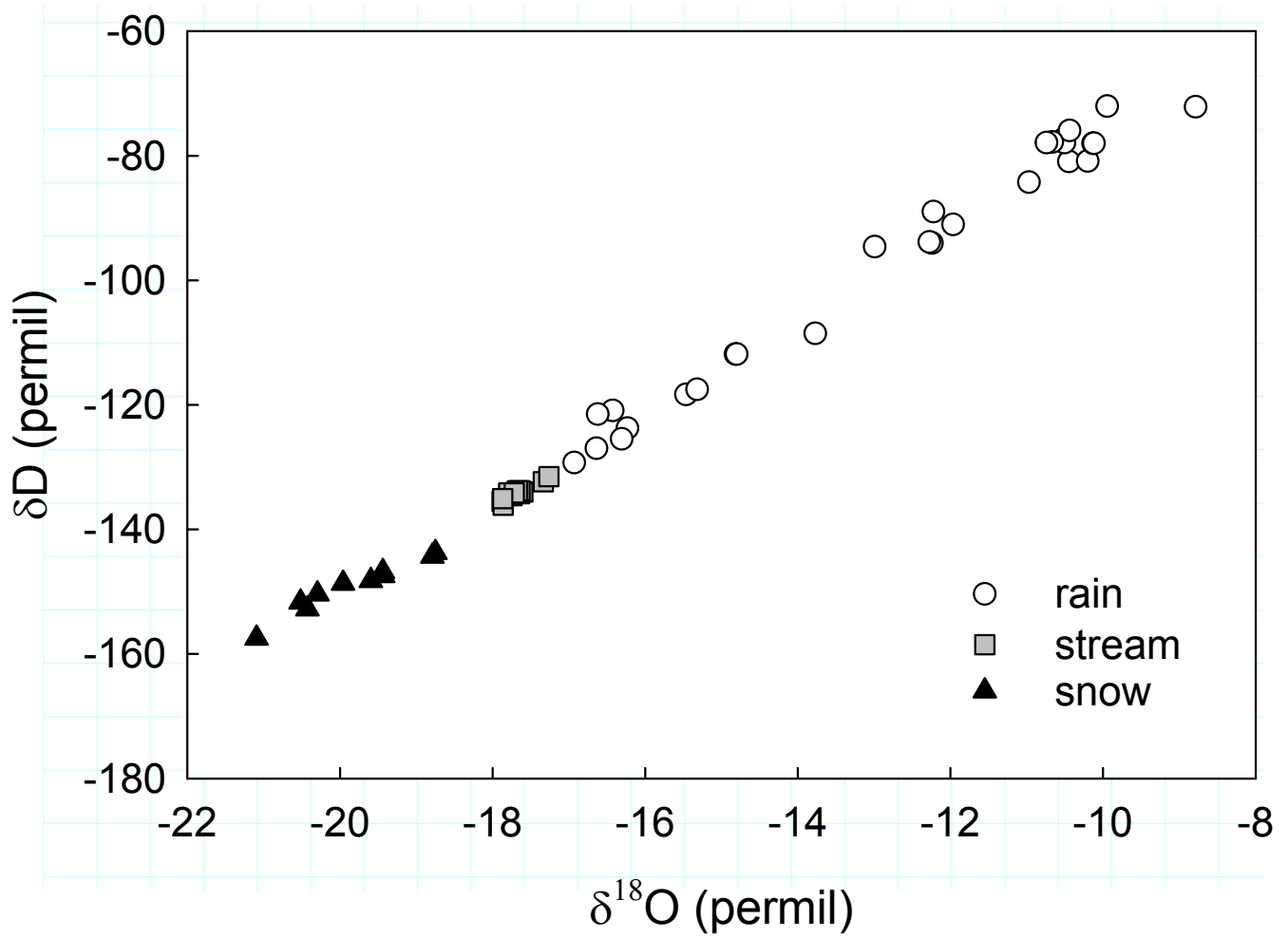


Figure 2: Local Meteoric Water Line [ref. pg. 3]

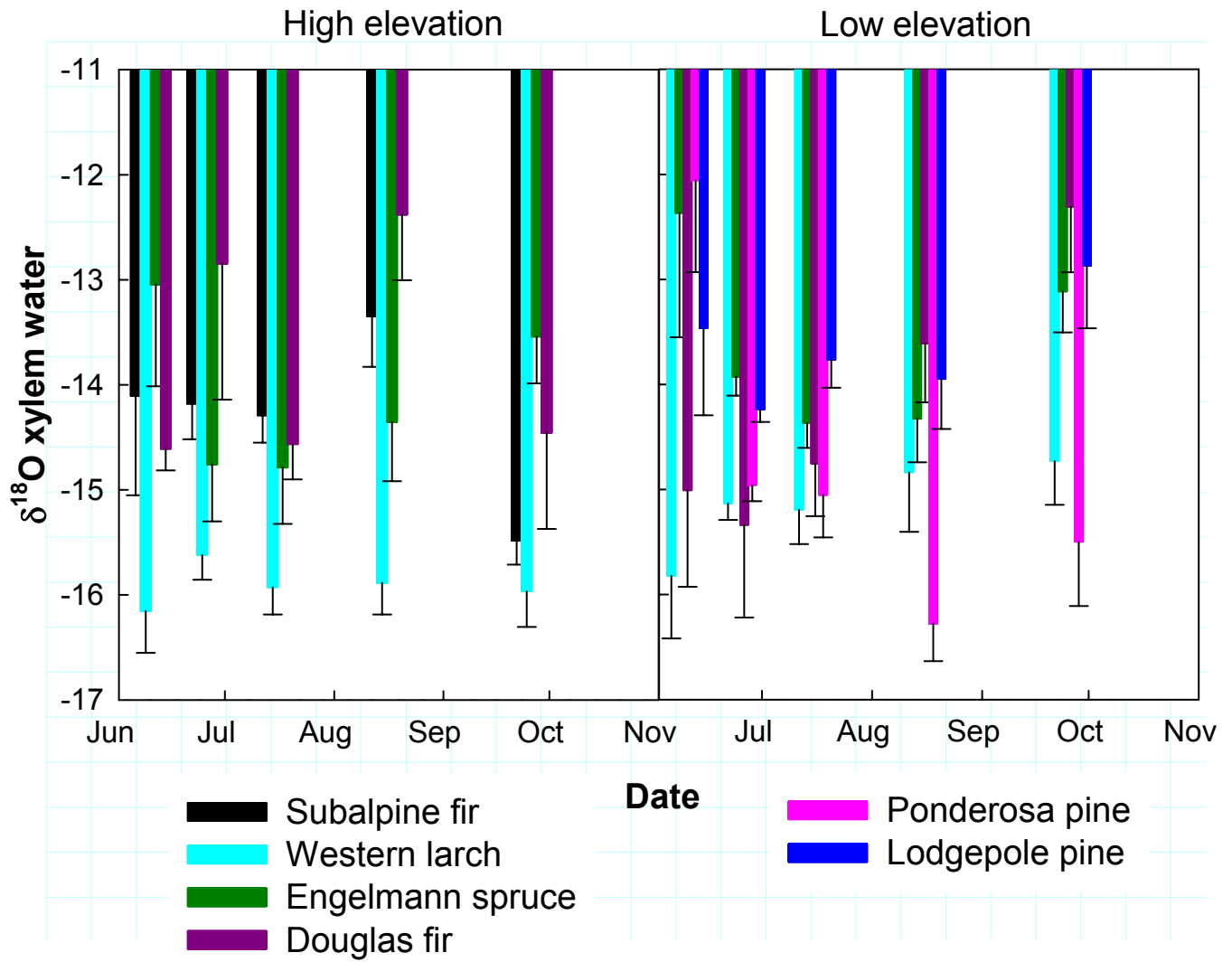


Figure 3: Species Differences in Xylem [ref. pg. 4]

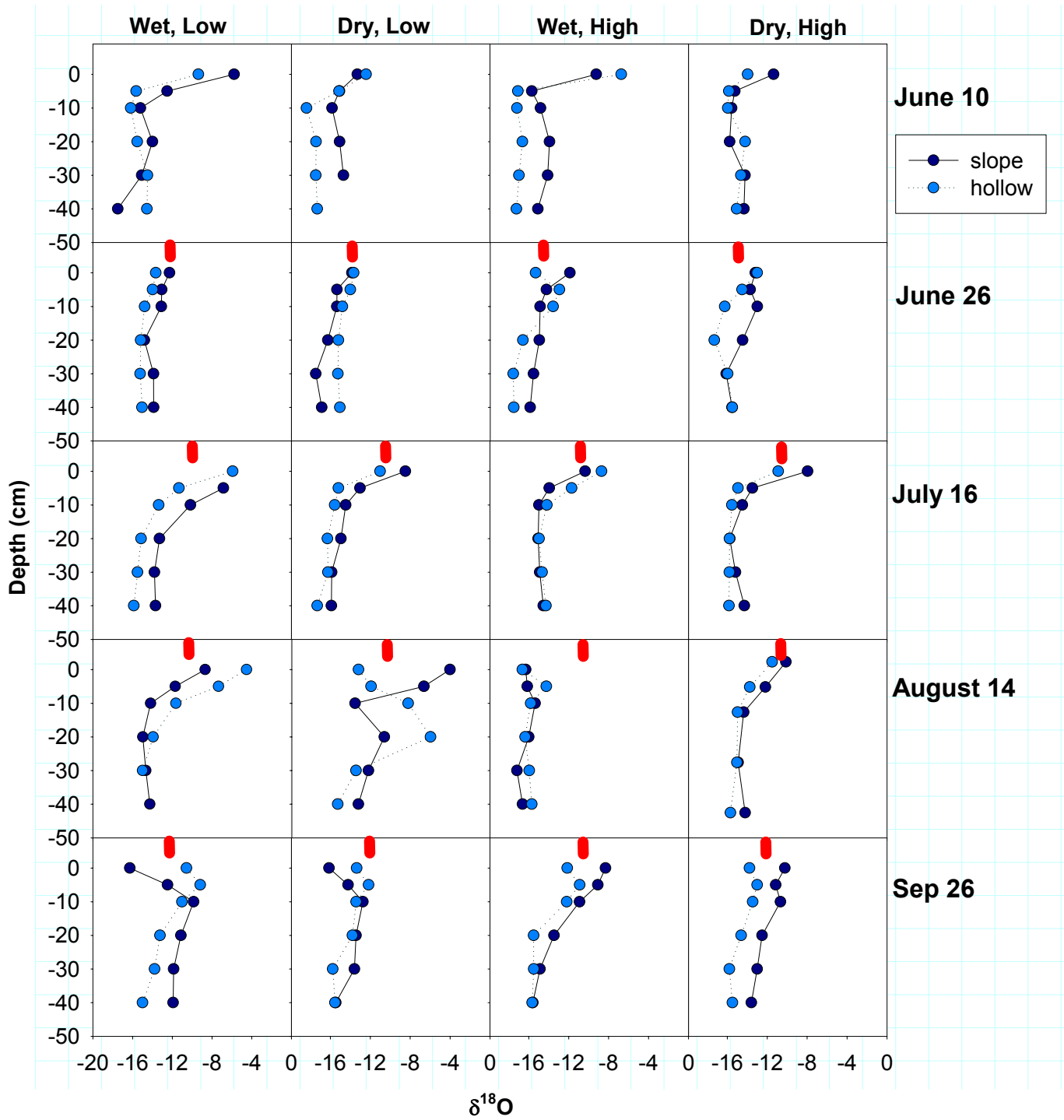


Figure 4: Soil Isotope Profiles [ref. pg. 4]

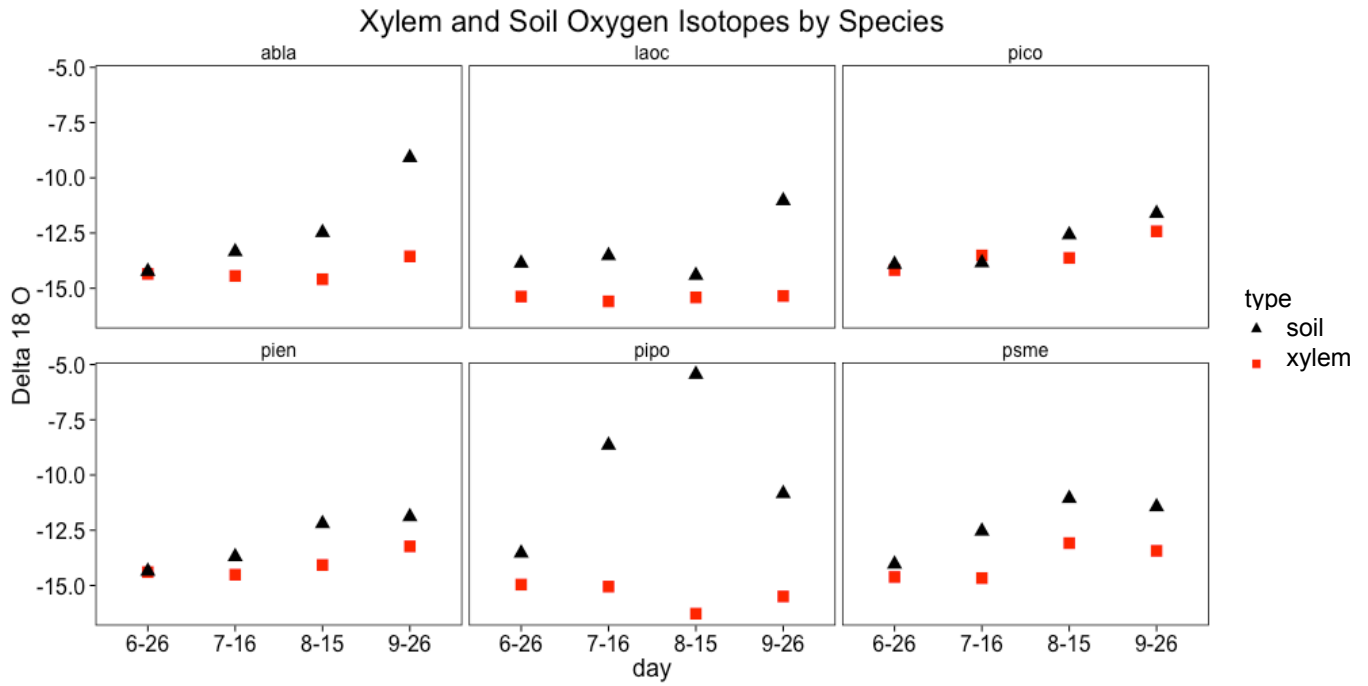


Figure 5: Species and Soil Isotopes [ref. pg. 4]

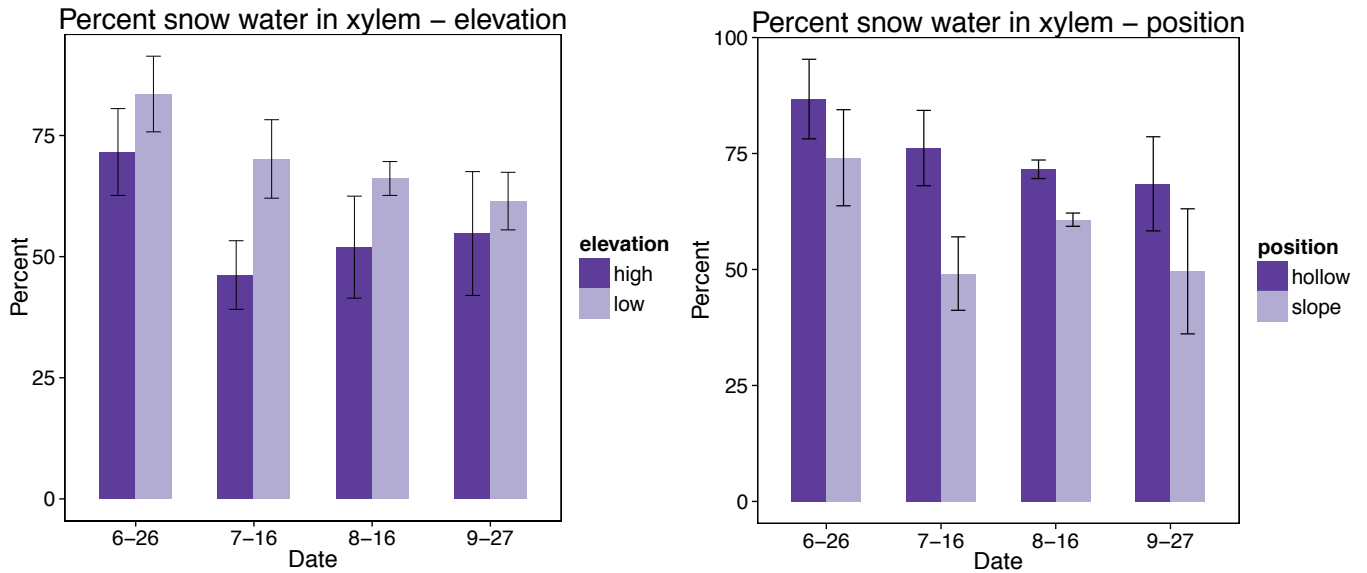


Figure 6: Topographic position vs. Percent Snow [ref. pg. 5]

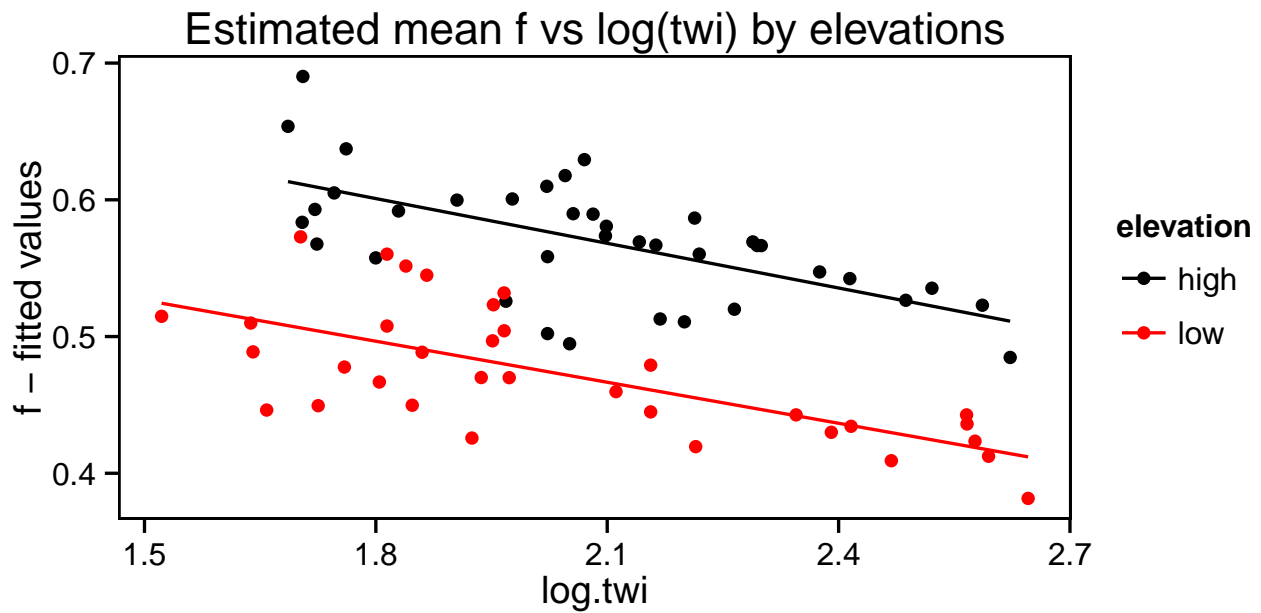
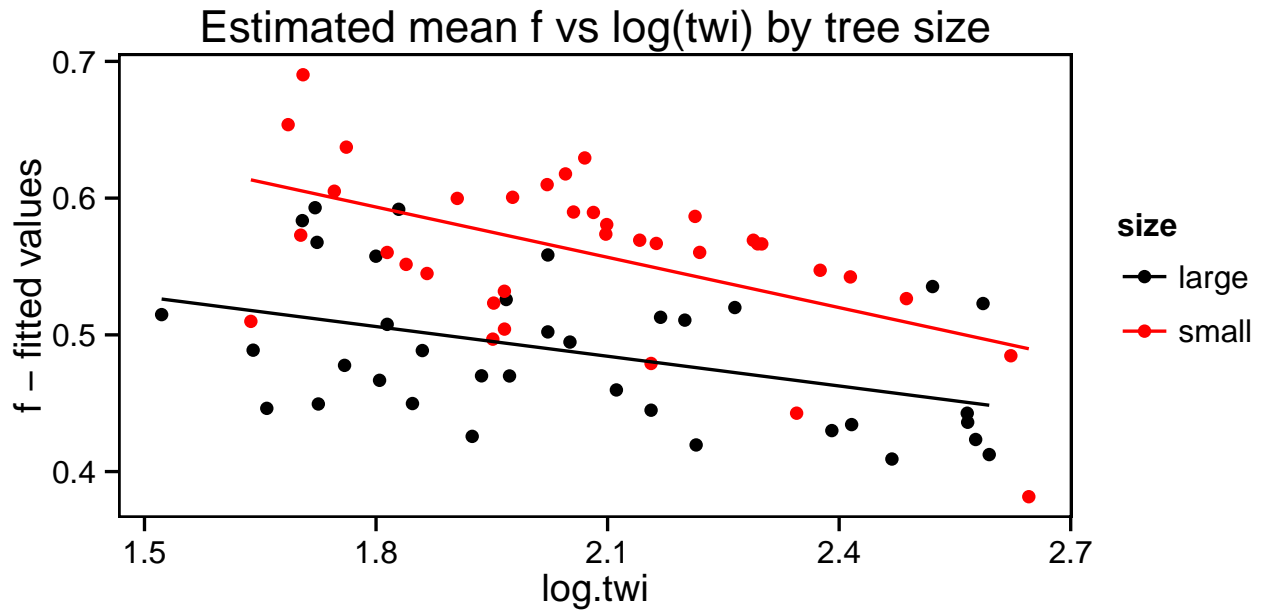


Figure 7: Fitted values vs twi [ref. pg. 5]

References

- [1] Pinde Fu and Paul M Rich. A geometric solar radiation model with applications in agriculture and forestry. *Computers and Electronics in Agriculture*, 37:25–35, 2002. [Cited on page 4.]

Student Fellowship: Conditions necessary to maintain chute-cutoff morphology in meandering gravel-bed rivers

Basic Information

Title:	Student Fellowship: Conditions necessary to maintain chute-cutoff morphology in meandering gravel-bed rivers
Project Number:	2014MT291B
Start Date:	3/1/2014
End Date:	2/28/2015
Funding Source:	104B
Congressional District:	MT 1
Research Category:	Climate and Hydrologic Processes
Focus Category:	Geomorphological Processes, None, None
Descriptors:	None
Principal Investigators:	April Sawyer

Publications

There are no publications.

Chute cutoff formation in wandering gravel-bed rivers

April M. Sawyer, M.S. Candidate, University of Montana, Geosciences

Montana Water Center Graduate Research Fellowship Final Report Summary

Overall Summary of Research to Date

My research has evolved to accommodate changes in methods, field study site and goals and objectives. First, I used a suite of 30 steady state model simulations along a rating curve and reconstructed hydrographs rather than highly computationally intensive unsteady model simulations. Second, I chose the Clark Fork River (CFR) at Milltown as a study site due to the 2011 cutoff event and Restoration Database (NRDP, 2013) availability, from which topography and bathymetry for modeling this large site was derived. Objectives are listed below. Last spring I collected data to calibrate a 2D model to use as a tool to investigate my research questions, including water surface elevation profiles at several flows, installing continuous water level loggers, velocity data collection by two methods, and field verification of surface grain size for sediment transport calculations. I attended a modeling training course last summer to improve my understanding of the governing equations and applications of the iRIC (USGS) modeling software.

Research Questions

The goals and objectives of this research are motivated by the following a) that chute cutoffs are indicative of the transition from meandering to braiding, and thus common in wandering gravel-bed rivers, b) that previous research has hypothesized chute cutoffs result as a function of interevent changes during a setup phase and intraevent changes during a trigger phase as modulated by magnitude and duration of flood events, and c) that much can be learned from an applied perspective by studying a restored river reach, where avulsions/cutoffs are often common. Various conceptual models of chute cutoff formation have been proposed but are poorly documented over a range of river systems, especially on wandering gravel-bed rivers. In this context, I have focused on the following questions:

- What are the spatial and temporal patterns of applied stresses exceeding sediment entrainment thresholds between main channel and overbank flow (cutoff) pathways?
- What is the role of duration in performing erosional work that could result in a chute cutoff?
- What are the differences between the bend that cutoff and the bends immediately upstream?

Results Summary

Figure 1 shows the predicted depth and velocity for the CFR site at and above the lower cutoff for four (of thirty) flow magnitudes (94.9 , 163 , 246 , and $360 \text{ m}^3\text{s}^{-1}$). Just above bankfull at $94.9 \text{ m}^3\text{s}^{-1}$, highest velocities are concentrated in the main channel, while side channels are only slightly inundated to $\sim 0.5 \text{ m}$ deep with velocities $< 1 \text{ m/s}$. As flows increase to 163 and $246 \text{ m}^3\text{s}^{-1}$, flow depth in the small constructed side channels connecting main channel meander bends increases exceeding 1 m . At these flows, localized side channel velocity exceeds 2 ms^{-1} in the lower cutoff and bend immediately upstream,

comparable to velocity magnitude in the main channel. These localized side channel high velocity zones exist in side channel meander apexes and at the upstream end where flow diverges from the main channel flow. At the peak of a moderately large flood event such as in 2011 ($360 \text{ m}^3\text{s}^{-1}$), the pattern of high ($\sim 2.5 \text{ ms}^{-1}$) velocity concentrated in moderately deep ($\sim 1 \text{ m}$) overbank flowpaths and side channels is very apparent. For the lower three meander bends with small side channels, these high velocity zones exist at the upstream end of the bar, or just downstream of the main channel meander apex upstream. Additionally, a large system of side channels conveying water on the river right floodplain re-joins the main channel just upstream of the lower cutoff bend. Finally, at the lower cutoff, total floodplain conveyance width reduces by over half, and the resultant increase in overbank velocities is apparent. Figure 2 shows the effect of narrowing total available floodplain cross section width as an increase in unit discharge (m^2/s ; discharge per unit 2 m cell width) conveyed along overbank flowpaths relative to the main channel. In these areas, shear stress capable of mobilizing the median grain size especially when persisting for long duration.

Wrapping Up

I am in the process of finishing up final post-processing and interpretation of model results for my thesis manuscript. I plan to defend my thesis later this summer after the draft has gone through review. I also plan to work with my advisor (Dr. Andrew Wilcox) to publish my manuscript in a peer-reviewed scientific journal relevant to water resources management or earth surface processes.

References

NRDP. 2013. Milltown Restoration Project Database. Prepared for the State of Montana Natural Resource Damage Program by River Design Group, Inc. Helena, MT. July, 2013.

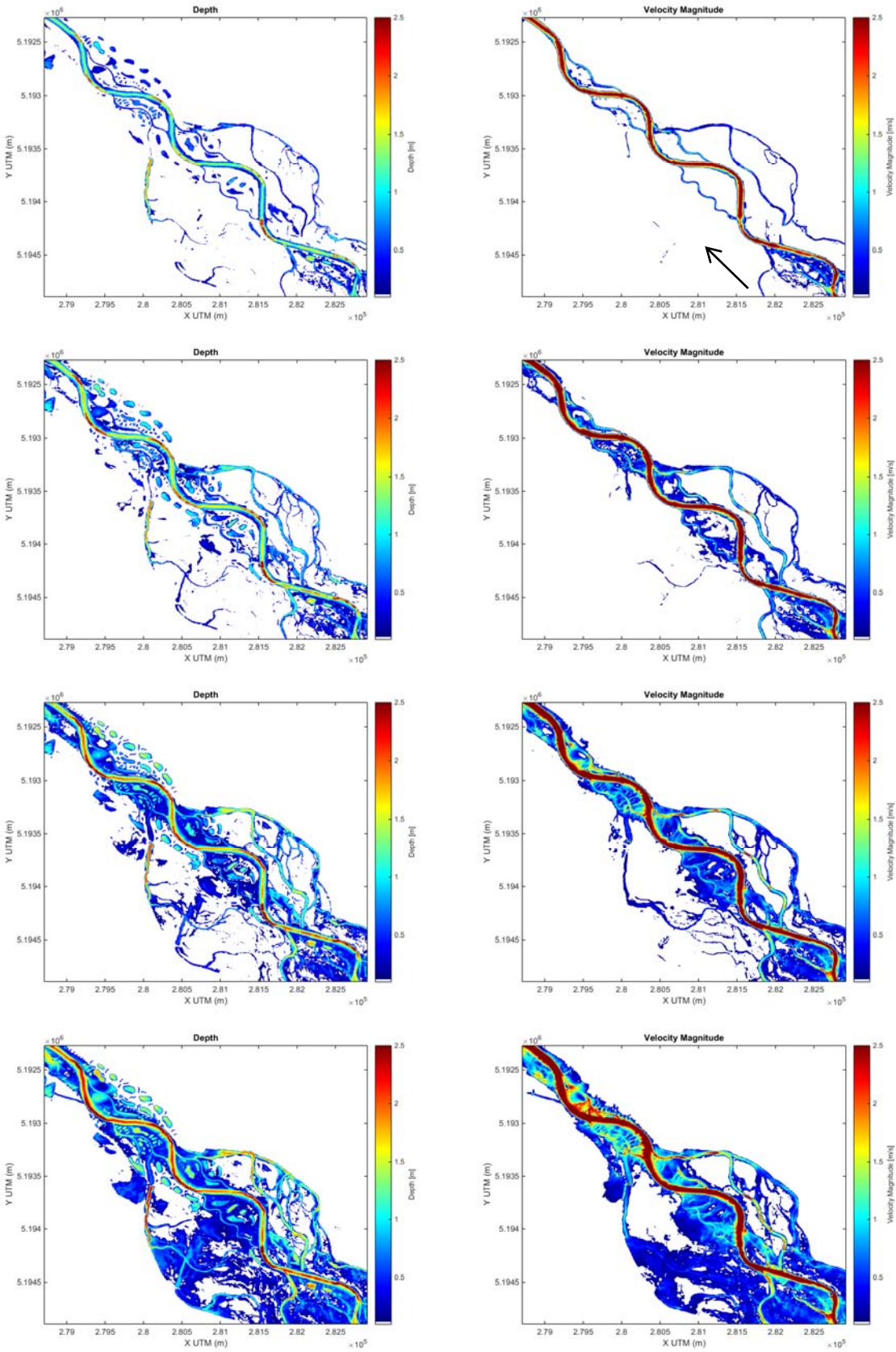


Figure 1. Modeled depth and velocity for four flows (94.9, 163, 246, and 360 m³s⁻¹) from approximately bankfull to the peak of the 2011 event; at and above the lower cutoff (upper left of images). Note high velocities concentrated in overbank areas at the lower cutoff location.

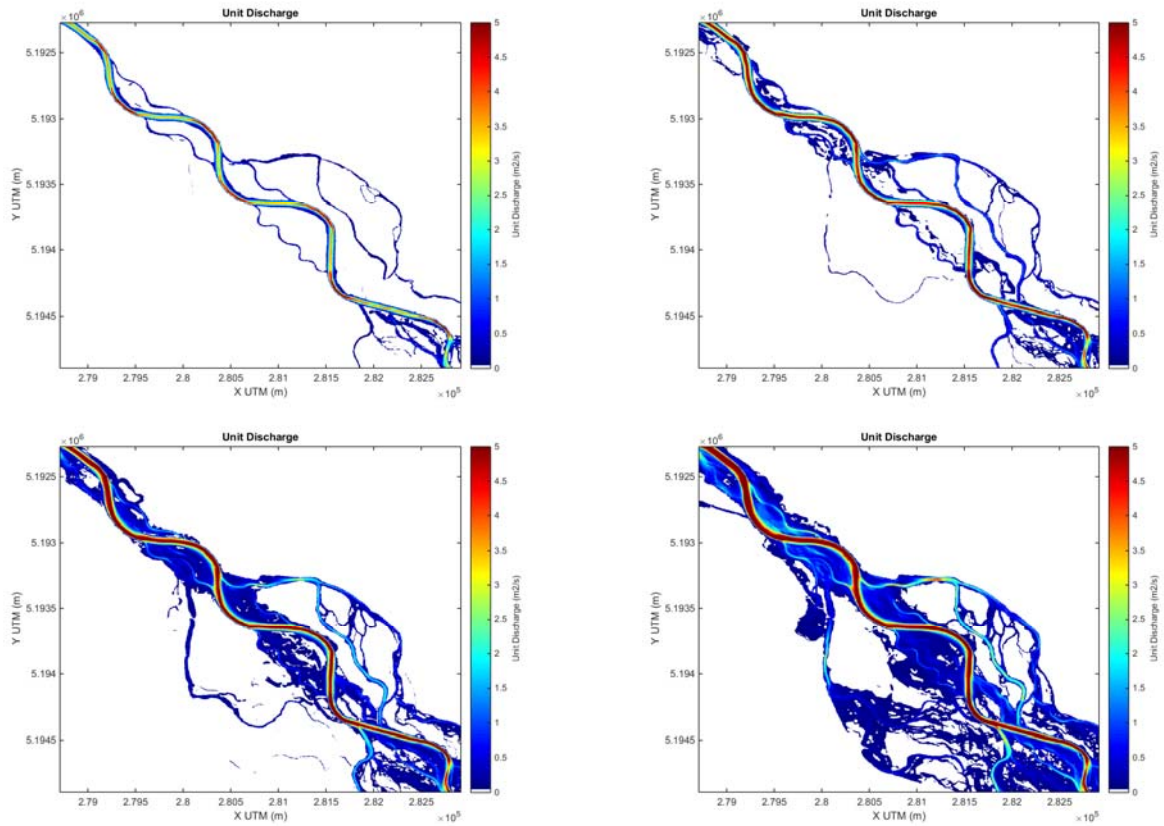


Figure 2. Unit discharge (flow per cell width or depth*velocity) for four flows (94.9, 163, 246, and 360 m^3/s) at and above the lower cutoff. Once more flow per unit width is concentrated in overbank areas as moderated by available overbank floodplain area, high shear stresses capable of sediment mobilization occur.

Information Transfer Program Introduction

Supporting students to become water science professionals is a core mission of the Montana Water Center. The center continued to work closely with faculty researchers to engage students in water-related research including producing reports and publishing papers. Faculty researchers who received research funding from the Water Center are required to actively mentor students in the research projects.

The Center encouraged students from a wide array of disciplines that are water related to apply for student fellowships. The Water Center also encouraged students engaged in water resource studies to present at regional and national conferences. The presentations and publications of faculty and students reported in their annual reports attests to the support given to students to both take on research and also present it at local and national meetings as well as follow through to publication in scientific journals.

In addition to working with faculty and students, Water Center programs reached thousands of others interested in water issues in Montana, including water resource professionals, teachers, farmers, ranchers, engineers, drinking water and wastewater system operators.

Education and outreach on various water topics was delivered to Montana citizens through the Montana Watercourse (MTWC), which is part of the Montana Water Center. MTWC provides hands-on, dynamic, water education through a series of diverse programs that target all levels of water users, youth through adults. Using practical, unbiased, legal, and scientific information, MTWC educates Montanans on basic water facts, water problems, and their solutions (mtwatercourse.org).

Specific information transfer activities include the following:

- * Published and distributed four Montana Water e-newsletters to approximately 1,600 professionals, students and decision makers concerned with water resource management.
- * Began development of a new website. It can be viewed at <http://www.montanawatercenter.org/>
- * The Montana Water Center continues to distribute training CDs funded by the EPA, for small drinking water systems titled Arsenic and Radionuclides: Small Water System Treatment Experiences.
- * Helped organize and execute a state water meeting with the Montana Section of the American Water Resources Association in Kalispell, MT on October 9-10, 2014. The conference theme was "Floods, Forests, and the Flathead". Approximately 160 people attended the conference with 43 speakers and 40 poster presentations. Oral and poster presentations highlighted much of the current water research being conducted throughout Montana by university, federal, state, county and non-profit researchers and resource managers. Director Wyatt Cross gave a welcoming address at the conference. The conference also had the usual good turnout of student presenters, representing the University of Montana, Montana Tech and Montana State University.
- * Responded to numerous information requests on water topics ranging from invasive water rights to importance of snowpack to Montanan's, to streamside setbacks to contaminants in Montana's surface and ground water, and ways to better manage these water sources.
- * Sponsored the 81st Annual School for Water & Wastewater Operators & Managers held in October 2013 at Montana State University. This training was attended by staff members of water and wastewater utilities with the purpose of preparing new system operators to pass the certification exam, and familiarize participants with other resources they may find helpful in the future. Director Wyatt Cross gave a welcoming address to the

Information Transfer Program Introduction

group.

*Offered a professional development course titled: “Wetland Regulations: Understanding Federal, State, and Local Regulations and the Permitting Process in Montana”. This was offered as a two-day, in-person course discussing rules and permitting regulations specific to Montana. Resource managers and educators joined the class, providing a multi-disciplinary perspective. Topic selection and planning of the 2015 professional development course is already in progress.

* Grant funded water education programs were delivered by MTWC that focused on the following areas: water rights trainings, dam owner workshops, water quality monitoring training, Project WET curriculum training, lake ecology graduate course, careers in water, and the Montanan Water supply Initiative material. Funding for these programs is provided through various grants including significant funding from Montana Department of Natural Resources and Conservation, and the Environmental Protection Agency.

USGS Summer Intern Program

None.

Student Support					
Category	Section 104 Base Grant	Section 104 NCGP Award	NIWR-USGS Internship	Supplemental Awards	Total
Undergraduate	2	0	0	0	2
Masters	5	0	0	0	5
Ph.D.	3	0	0	0	3
Post-Doc.	0	0	0	0	0
Total	10	0	0	0	10

Notable Awards and Achievements

Duncan Patten, the director of the Montana Water Center, stepped down from his position in June of 2014. Duncan was awarded an outstanding service award from NIWR.

Publications from Prior Years

1. 2011MT241B ("Using ^{222}Rn and Isotopic Tracers to Trace Groundwater-Lake Interactions") - Other Publications - Shaw, Glenn, and Elizabeth White, (2013) Nutrients and Groundwater-Lake Interactions at Georgetown Lake, MT, Montana Department of Environmental Quality Report, pp. 30., (In Review).
2. 2013MT281B ("Student Fellowship: Maintaining Migratory Pathways of Imperiled Large River and Small Stream Prairie Fishes in the Face of Climate Change") - Dissertations - Dockery, David. 2015. RELATIONSHIPS AMONG SWIMMING PERFORMANCE, BEHAVIOR, WATER VELOCITY, TEMPERATURE, AND BODY SIZE FOR SAUGER SANDER CANADENSIS AND LONGNOSE DACE RHINICHTHYS CATARACTAE. "Ph.D Dissertation," Fish and Wildlife Management, Montana State University, Bozeman, Montana, 137 pages.
3. 2010MT224B ("Student Fellowship: Fine Sediment Infiltration and Sediment Routing in the Clark Fork River, Montana") - Articles in Refereed Scientific Journals - Evans, E. and A. C. Wilcox 2013, Fine-sediment infiltration dynamics in a gravel-bed river following a sediment pulse, River Research and Applications doi: 10.1002/rra.2647.
4. 2012MT276B ("Student Research Fellowship: The Effect of Physiographic Parameters on the Spatial Distribution of Snow Water Equivalent: an Analysis of the Representativeness of the Lone Mountain SNOTEL Site") - Dissertations - Wetlaufer, Karl, 2013, The effect of basin physiography on the spatial distribution of snow water equivalent and snow density near peak accumulation by, "M.S. thesis," Earth Sciences, Montana State University, Bozeman, Montana, 113 pages.
5. 2011MT241B ("Using ^{222}Rn and Isotopic Tracers to Trace Groundwater-Lake Interactions") - Dissertations - Mitchell, Katie, 2014, Groundwater and Surface Water Interactions at Georgetown Lake, Montana with Emphasis on Quantification of Groundwater Contribution, "M.S. Thesis," Montana Tech of the University of Montana, Butte, Montana, 70 pages.
6. 2011MT244B ("Student Fellowship: Population-scale effects of hypoxia on the distribution and abundance of fishes in Silver Bow Creek") - Other Publications - McMahon, T.E., R.G. Gresswell, M.P. Mayfield, and J.P. Naughton, 2013, Fisheries and water quality response to Superfund remediation in Silver Bow Creek and the upper Clark Fork River, Montana, Final Reports to Natural Resources Damage Program, Montana Dept of Justice, and Montana Fish, Wildlife and Parks